PERINATAL ORGANOPHOSPHATE FLAME RETARDANT EXPOSURE ALTERS ADULT HPA AXIS FUNCTION AND AVOIDANCE BEHAVIOR IN A SEX-SPECIFIC MANNER IN MICE

Catherine M. Rojas[a], Julia DeLucca[b], Caylee A, Brown[a], Ali Yasrebi[b], Savannah Chiou[b], Nicholas T. Bello[b], Troy A. Roepke[a,b]

Affiliations:

[a] *Joint Graduate Program in Toxicology, Rutgers, The State University of New Jersey, Piscataway, NJ 08854, USA*

[b] *Department of Animal Sciences, School of Environmental & Biological Sciences, Rutgers, The State University of New Jersey, New Brunswick, NJ 08901, USA*

Corresponding Author:

T.A. Roepke. Department of Animal Sciences, School of Environmental and Biological Sciences, Rutgers, The State University of New Jersey, 84 Lipman Drive, Bartlett Hall, New Brunswick, NJ, 08901, USA. E-mail address: ta.roepke@rutgers.edu. Phone: (848) 932-9454

Keywords:

flame retardants, endocrine disruption, acute stress, HPA axis

Abbreviations

EPM, Elevated Plus Maze; GD, Gestational Day; LDB, Light-Dark Box; OFT, Open Field Test; OPFR, Organophosphate Flame Retardants; PBDE, Polybrominated Diphenyl Ether; PND,

postnatal day; TCP, Tricresyl Phosphate; TDCPP, Tris(1,3-dichloro-2-propyl) phosphate; TPP, Triphenyl Phosphate.

Abstract

Organophosphate flame retardants (OPFRs) are ubiquitous flame-retardant additives with endocrine-disrupting properties. Despite increasing evidence that OPFRs impact neurodevelopment, their effects on the neuroendocrine stress response remain poorly understood. To examine their long-term impact on stress regulation, we treated pregnant C57Bl/6J dams to a mixture of tris(1,3-dichloro-2-propyl) phosphate (TDCPP), triphenyl phosphate (TPP), and tricresyl phosphate (TCP; 1 mg/kg each) from gestational day (GD) 7 through postnatal day (PND) 14. Adult offspring (8-9 weeks of age) were then challenged with acute stressors, including 1 h restraint or a 6-day acute variable stress (AVS) paradigm. Perinatal OPFR exposure produced persistent, sex-specific alterations in the hypothalamic–pituitary–adrenal (HPA) axis and stress-related neurocircuitry. Following 1 h restraint, OPFR-treated females showed heightened serum corticosterone. In addition, gene expression analysis revealed sex-dependent disruptions in key stress-regulatory pathways after OPFR treatment and 1 h restraint in the hypothalamus (*Crhr1, Crhr2, Ptpn5*) and pituitary (*Crhr1, Pomc, Nr3c1*). Females demonstrated more differences in adrenal gene expression related to steroidogenesis (*Mc2r, Cyp11b2*) and catecholamine biosynthesis (*Dbh, Pnmt*), with OPFR-treated groups having blunted responses. OPFR AVS females displayed reduced corticosterone and downregulated *Pacap/Pac1r* expression in the bed nucleus of the stria terminalis (BNST), accompanied by increased behavioral avoidance and immobility. In males, OPFR exposure led to increased BNST *Pacap* and *Pac1r*, expression, along with hyperactivity and avoidance behaviors. Together, these findings demonstrate that early-life OPFR exposure induces lasting, sex-specific dysregulation of the HPA axis and associated stress circuits, highlighting OPFRs as developmental neuroendocrine disruptors with implications for mood and stress-related disorders.

Introduction

The worldwide production of flame retardants has increased to more than 2.39 million tons in 2019 (1). There has been increased usage of flame retardants to adhere to fire safety regulations. While many organohalogen flame retardants, such as polybrominated diphenyl ethers (PBDEs) have been phased out due to overt toxicity and bioaccumulation, organophosphate flame retardants (OPFRs) continue to be used as a "regrettable substitution" (2). OPFRs are a class of endocrine-disrupting chemicals (EDCs) that have demonstrated deleterious effects on neural development, reproduction, and brain and thyroid function (3-6). OPFRs have low degradation potential and persist in household dust since they are not chemically bound to products like furniture, mattresses, and children's products (7). As a result, vulnerable populations are exposed to OPFRs, particularly children who have had 4-5x higher levels of urinary OPFR metabolites compared to their mother which has been associated with adverse neurological outcomes (8,9).

Disruptions in neurological development have been linked to mood disorders and maladaptive behaviors (10). Perinatal exposure to OPFRs have shown to affect neurological development through disrupting neurogenesis, synaptogenesis, and neurotransmission (11). Epidemiological studies have shown that combined exposure to OPFRs is significantly associated with the increased risk of depression (12). In addition, positive associations of prenatal exposure to organophosphate esters (OPEs) has been associated with greater behavioral problem scores in children from mothers with pregnancy-related anxiety (13). There is limited research on how OPFRs specifically affect the neuronal pathways responsible for regulating stress responses. No studies to date have looked at how perinatal OPFR treatment in mice can alter the development of the major stress response pathway, the hypothalamic-pituitary-adrenal (HPA) axis.

92 Upon activation of the HPA axis by external stressors, the paraventricular nucleus of the
93 hypothalamus (PVN) synthesizes and releases corticotrophin releasing hormone (CRH) at the
94 median eminence which enters the hypophyseal portal blood system and reaches the anterior
95 pituitary (14). CRH binds and activates CRH-receptor 1 (CRHR1), the main receptor responsible
96 for mediating HPA axis activation at the level of the pituitary. CRHR1 increases pro-
97 opiomelanocortin (POMC) transcription which is post-translationally cleaved to form
98 Adrenocorticotropin Hormone (ACTH). ACTH is secreted from the anterior pituitary corticotrope
99 cells and directly binds to melanocortin 2 receptor (MC2R) located on the surface of the adrenal
100 zona fasciculata cells. ACTH signaling stimulates an increase in precursor cholesterol for
101 steroidogenesis by: increasing *de novo* cellular cholesterol synthesis, mobilizing cholesterol esters
102 stored in lipid droplets, and increasing low-density-lipoprotein (LDL) receptor-mediated
103 cholesterol uptake (15). Most importantly, ACTH signaling initiates the activation of the single
104 steroidogenic rate limiting step, the conversion of free cholesterol to pregnenolone by CYP11A1.
105 The adrenal glands are responsible for producing and releasing hormones during the stress
106 response. Glucocorticoid production in the adrenal zona fasciculata is species-specific; while
107 humans primarily produce cortisol, rats and mice predominantly produce corticosterone (CORT)
108 due to poor expression of CYP17 (15). In parallel, the adrenal medulla's chromaffin cells rapidly
109 synthesize and release catecholamines as part of the Sympathetic-Adreno-Medullary (SAM) axis.
110 In response to external stressors detected by the brainstem, sympathetic preganglionic neurons in
111 the thoracic spinal cord that innervate the adrenal medulla trigger the release of norepinephrine
112 and epinephrine (adrenaline) (16). Glucocorticoids further amplify this response, as cortisol/CORT
113 enhances phenylethanolamine-N-methyltransferase (*Pnmt*) activity, an enzyme that converts

114 norepinephrine to epinephrine (17). Therefore, both axes are essential for mounting a proper stress
115 response through creating a positive bidirectional feedback loop.

116 An essential mechanism of the stress response is the system of negative feedback loops
117 that restore HPA activity to pre-stress conditions. Long feedback loops involve CORT-mediated
118 inhibition of corticotropin-releasing hormone (CRH) synthesis and secretion in the hypothalamus,
119 as well as suppression of adrenocorticotropic hormone (ACTH) synthesis in the pituitary. Various
120 short feedback loops also exist, such as ACTH-mediated inhibition of CRH synthesis in the adrenal
121 glands (14,18). Glucocorticoid receptors (GRs) further regulate these feedback mechanisms,
122 facilitating termination of the stress response (19). Organophosphate flame retardants (OPFRs)
123 have been shown to antagonize GR activity and disrupt steroidogenesis in human adrenocortical
124 carcinoma (H295R) cells (20-22). Rodent studies likewise report alterations in adrenal size and
125 function following OPFR exposure (23-26), suggesting that OPFRs may interfere with HPA axis
126 regulation. However, no studies have examined how perinatal OPFR exposure affects HPA activity
127 in adulthood. Dysregulation of the stress response is linked to the pathophysiology of stress-related
128 mood disorders, which are more prevalent in females (27,28). We therefore hypothesized that
129 perinatal OPFR exposure would disrupt the adult HPA axis response to acute stressors, with female
130 mice having increased susceptibility.

131 Acute stressors, such as immobilization or foot shock, are well documented to elevate
132 circulating corticosterone in rodents (29). Furthermore, acute or subchronic variable stress
133 paradigms are widely used to model anxiety- and depression-like behaviors in rodent studies (30).
134 Notably, sex differences in these responses have been documented, likely reflecting the distinct
135 roles of androgens and estrogens in hypothalamic–pituitary–adrenal (HPA) axis regulation and the
136 overlapping distribution of gonadal and steroid receptors within stress-related neural circuits

137 (28,31). Our laboratory has likewise observed sex-dependent effects of chronic stress on behavior,
138 neuronal activity, and the central stress transcriptome in males and in females dependent on estrous
139 stage (32-34). Given that organophosphate flame retardants (OPFRs) can disrupt both neural
140 development and hormonal signaling, these findings raise the question of whether perinatal OPFR
141 exposure similarly alters central stress responses in a sex-specific manner.
142
143 **Materials and Methods**
144 Animal Care
145 All animal treatments and procedures were completed in accordance with National Institutes of
146 Health guidelines, the Rutgers Institutional Animal Care and Use Committee, and the ARRIVE
147 guidelines for reporting animal research. Wild-type (WT) C57Bl/6J (Jackson Laboratory), both
148 female and male, were bred in-house and maintained under controlled conditions: temperature
149 (25°C), humidity (30-70%), and a 12 h light/dark cycle. Mice had *ad libitum* access to water and
150 a standard, low-phytoestrogen chow diet (Lab Diets, 5V75). Females were identified by the
151 presence of a vagina and an estrous cycle, and males were identified by the presence of a penis
152 and scrotal sac and larger anogenital distance.
153
154 Flame retardants
155 The OPFR mixture we have used previously (35,36) includes tricresyl phosphate (TCP,
156 AccuStandard, New Haven, CT, CAS#:1330-78-5, 99%), tris(1,3-dichloro-2-propyl)phosphate
157 (TDCPP, Sigma Aldrich, St. Louis, MO, CAS#:13674-87-8, 95.6%), and triphenyl phosphate
158 (TPP, Sigma Aldrich, St. Louis, MO; CAS#:115-86-6, 99%). For the mixture, 100 mg of each

159 OPFR were dissolved in 1 ml of acetone (Sigma-Aldrich), then 100 µl of acetone stock solution
160 was added to 10 ml sesame oil and allowed to vent for 48 h.
161
162 Experimental Design
163 Females were pair-housed with males for 1 week. Gestational day (GD) 0 was confirmed by the
164 presence of a vaginal plug. Dams were weighed every 3 days to adjust dosing concentrations and
165 were randomly assigned to treatment groups: sesame oil vehicle combined with powdered peanut
166 butter (PB2®, PB2 Foods) or OPFR mixture (see below for preparation of mixture) in sesame oil
167 combined with powdered peanut butter. Dosing was orally administered at 1 mg of each
168 OPFR/kg bodyweight/day daily from GD 7 to post-natal day (PND) 14.
169 Due to limited knowledge of OPFR effects on the stress response, the first set of
170 experiments that were conducted utilized a single acute stressor. From each litter, 2 male and 2
171 female pups were weaned at PND 21. One male or female were assigned to a control
172 (unstressed) group, and their littermates to the restraint group. Control and restrained mice were
173 housed separately, regardless of maternal treatment. All offspring were maintained on a standard,
174 low-phytoestrogen chow diet (Lab Diets, 5V75) and housed *with ad libitum* access to food and
175 water. At 7-8 weeks of age, both control and restrained mice were handled daily for 5 min during
176 the week prior to sacrifice. At 8-9 weeks of age, restrained mice were subjected to 1 h of restraint
177 stress using a 50 mL conical tube and euthanized immediately afterwards. All mice were
178 euthanized by decapitation between 1000-1130 h, with control mice being euthanized before
179 restrained mice. The 1 h restraint study included the following experimental groups and animals
180 used: male:oil:con- 13, male:oil:restrained- 11, male:OPFR:con- 11, male:OPFR:restrained- 11,

181 female:oil:con- 11, female:oil:restrained- 11, female:OPFR:con- 14, and
182 female:OPFR:restrained- 12.
183 The next set of experiments utilized an acute variable stress (AVS) paradigm. Pups from
184 each litter (2 males and 2 females) were weaned at PND 21. One male or female were assigned
185 to a control (unstressed) group, and their single littermate to the acute variable stress (AVS)
186 group. Control and AVS mice were housed separately, regardless of maternal treatment. All
187 offspring were maintained on a standard, low-phytoestrogen chow diet (Lab Diets, 5V75) and
188 housed with *ad libitum* access to food and water. At 7-8 weeks of age, control mice were handled
189 daily for 5 min for 6 days leading up to behavior testing. Experimental mice were exposed to a 6-
190 day AVS paradigm (described below). Behavior testing was conducted from Day 7 – Day 10 in
191 the following order: open field test (OFT), elevated plus maze (EPM), light/dark box emergence
192 test (LDB), and novelty suppressed feeding (NSF) (see below for more details). On Day 11, all
193 mice were euthanized by decapitation between 1000-1130 h, with control mice being euthanized
194 before AVS mice. This study included the following experimental groups and animals used:
195 male:oil:con- 13, male:oil:AVS- 12, male:OPFR:con- 12, male:OPFR:AVS- 12, female:oil:con-
196 12, female:oil:AVS- 12, female:OPFR:con- 15, and female:OPFR:AVS- 15. One oil-treated AVS
197 female mouse died during the last stressor in the startle box chamber. Their weight was
198 consistent with the previous week, and their right eye was cloudy, thus, their death was most
199 likely stemmed from other internal complications. All other mice were in good health (according
200 to IACUC guidelines) and did not lose weight a significant amount of weight until NSF testing.
201
202 Acute Variable Stress Paradigm

203 We reviewed the literature for physiological stressors that were commonly used in acute stress or
204 fear-inducing paradigms to create our novel paradigm (30,37,38). Day 1 was 1 h restraint using a
205 50mL conical tube which was placed in their home cage. Day 2 was 1 h cold stress at 4°C in a
206 fridge only intended for animal use. Day 3 was 1 h platform shake at 100 rpm using a modified
207 orbital plate shaker. Day 4 was 1 h restraint and day 5 was 1 h platform shake. Day 6 was 30 min
208 of sound stress using a startle box (MedAssociates; 12,000Hz/105dB/30 ms). The stressors were
209 repeated randomly so that the same stressor was not done two days in a row. The last stressor
210 was sound stress since we wanted to collect startle response data to observe differences in
211 treatment and sex (Fig. S6).
212
213 Behavior assays
214 Adult male offspring were tested before female offspring each day of testing. Mice were
215 acclimated to the behavior room for at least 24 h prior to the first test. OFT was conducted first
216 as it is the least stressful, EPM was conducted second to allow for washout between the OFT and
217 LDB since they are conducted in the same apparatus, and NSF was conducted last to avoid
218 confounding effects of food deprivation on other tests. The OFT apparatus measures 40 cm long
219 x 40 cm wide x 40 cm high with an open top and a 64-square grid floor. The mice were placed on
220 the bottom left corner of the arena at the start of the test and the ANY-maze software measured
221 activity in the perimeter, corners, 20 cm center, and 10 cm center for 10 min. The EPM apparatus
222 has 4 arms which are 30 cm long x 5 cm wide which all intersect at the 5 cm square center. The
223 walls that enclose 2 of the arms are 15 cm tall with open tops. The mice were placed into the
224 center of the apparatus at the start of the test and the ANY-maze software measured activity in
225 open arms, closed arms, and center.

226 The LDB test is conducted in the OFT apparatus with a black insert that is 20 cm long x
227 40 cm wide x 40 cm tall. The mice are placed on the bottom left corner of the arena and the
228 ANY-maze software measured activity in the light zone, transition zone, and dark zone. Although
229 there is no camera inside the dark portion of the apparatus, the software can still measure entries,
230 exits, and time spent. The NSF is conducted in a white rectangular box with an open top (30 cm
231 long x 50 cm wide x 16 cm tall) and fresh bedding. The center of the arena contains a pedestal
232 (10 cm diameter) with a fresh food pellet attached. The mice were placed into the bottom left
233 corner of the arena and the ANY-maze software measured how long it took for the mice to eat.
234 Once the mice eat, or 10 minutes have elapsed without eating, the mice are then placed in their
235 home cage for 5 min.

236 The OFT, EPM, and LDB chambers were cleaned with MB-10 (Quip labs) spray in
237 between each animal to ensure that behavior was not influenced by scent. The novel area for
238 NSF was raked in between each animal, and the apparatus was cleaned with MB-10 and fresh
239 bedding was added before female mice were tested. The NSF pedestal was also cleaned in
240 between each animal, with the paper disk and pellet being changed for female mice. All tests
241 were recorded and analyzed by the ANY-Maze behavior monitoring software (ANY-Maze,
242 Version 6, Stoelting, USA). Vaginal cytology was performed on the female offspring after each
243 test to confirm estrous stage.

244 Exclusion criteria for each test included mice that did not enter all zones at least once or
245 if the test did not reach full duration. We excluded one mouse from OFT because there were
246 technical issues where the test ended early by accident. We excluded one OPFR AVS female
247 mouse in EPM because they only entered one closed arm and stayed in the same spot for the
248 duration of the test (this same mouse also did not eat in the novel arena). We excluded one mouse

249 for LDB because there were technical issues where the test ended early by accident. We excluded
250 one cohort of mice (12 mice) from NSF because their cages were not changed the day before
251 which caused most of the mice to not eat in the novel area or home cage. Although their food
252 was removed the day prior, the mice most likely ate their feces or small pellets of food that fell
253 onto the bottom of their cage.
254
255 Tissue preparation and quantitative real-time PCR
256 Sections of the paraventricular nucleus of the hypothalamus (PVN) and anterodorsal bed nucleus
257 of the stria terminalis (adBNST) were microdissected from adult offspring under a dissecting
258 microscope as previously described (35). The pituitary (both anterior and posterior) and both
259 adrenal glands were collected for RNA extraction as well. All tissues were stored in RNALater
260 (Life Technologies, Grand Island, NY) at -80°C, and RNA was extracted using RNAqueous-
261 Micro Kits, Life Technologies. RNA quantity and quality were assessed using a NanoDrop-2000
262 spectrophotometer (ThermoFisher, Waltham, MA) and RIN was determined using an RNA 6000
263 Nano kit on an Agilent Bioanalyzer. cDNA was synthesized as previously described (39) and 4
264 µl of cDNA was amplified by either Power SYBR Green (ThermoFisher) or SSO Advanced
265 (BioRad, Hercules, CA) Master Mix. Refer to supplemental tables 1 and 2 for the complete list
266 of primer sequences used in these experiments. Relative gene expression was determined using
267 the δδCT method calculated by the geomean of reference genes *Actb*, *Gapdh,* and *Hprt*.
268
269 Corticosterone Assay
270 Trunk blood was collected immediately following decapitation and kept at room temperature for
271 at least 30 min. Serum was then isolated, collected, and stored at -80°C for CORT level analysis.

272 CORT levels were measured using an ELISA kit (RTC002R; BioVendor) with the lower limit of
273 detection being 6.1 ng/mL. The intra-assay coefficient of variation range was 5.9%–8.9% and the
274 inter-assay coefficient of variation range was 7.2%–7.5%. For analysis, a logarithmic regression
275 was used to convert absorbance values to concentrations in ng/ml.
276
277 Data Analysis
278 Data were stratified by sex and analyzed by 2-way ANOVA (maternal treatment and adult
279 exposure) followed by Fisher's LSD post-hoc comparison as we were only interested in within
280 treatment differences using GraphPad Prism 10 (San Diego, CA). Kaplan-Meier survival curves
281 were analyzed by Log-rank test. All gene expression data were normalized to the oil control
282 group within each sex. Outliers were determined using the Grubbs test, and values that exceeded
283 3 SDs ($\alpha<0.01$) above or below the group mean were excluded. Results were considered
284 statistically significant at $\alpha<0.05$ and data are represented as mean ± SEM.
285
286 **Results**
287 For the following findings, all treatment effects reported are effects of perinatal OPFR treatment
288 and all exposure effects reported are effects of adult restraint or AVS exposure.
289
290 *Corticosterone and epinephrine measurement after 1 h restraint*
291 CORT analysis revealed an effect of exposure [$F(1,27)=11.33$, $P=0.0023$] where OPFR
292 restrained females had increased levels compared to OPFR control females ($P<0.01$) (Fig. 1A).
293 There was also an exposure effect in male mice [$F(1,25)=93.91$, $P<0.0001$] where restrained
294 mice had higher levels of CORT compared to control mice across treatment groups ($P<0.0001$)

295 (Fig. 1C). No differences in serum epinephrine concentrations were observed across treatment or
296 exposure groups (Fig. 1B and 1D). Overall, perinatal OPFR treatment and restraint stress
297 increased circulating corticosterone levels in both sexes
298
299 *OPFR treatment altered stress-related genes in the PVN*
300 We selected genes that are part of the central stress response pathway. In females, there was an
301 exposure effect for *Crh* expression [F(1,27)=4.685, P=0.0394] (Fig. 2A). A treatment effect was
302 seen for *Crhr1* expression in females [F(1,28)=5.729, P=0.0236] (Fig. 2B). An exposure effect
303 was seen in female *Crhr2* expression [F(1, 28)=7.198, P=0.0121], with an increase in OPFR
304 restrained group compared to OPFR control group (P<0.05) and a trending decrease in OPFR
305 control mice compared to oil control (P=0.0526; Fig. 2C). No differences were noted for *Pacap*
306 expression across all groups (Fig. 2D). *Pac1r* expression was affected by treatment
307 [F(1,26)=7.692, P=0.0101], with a decrease in expression in OPFR restrained females compared
308 to oil restrained females (P<0.05; Fig. 2E). In addition, *Ptpn5* expression was affected by
309 treatment [F(1,27)=8.846, P=0.0061] where there was an increase in expression in OPFR control
310 females compared to oil control females (P<0.01; Fig. 2F).
311 In males, no differences were seen in *Crh, Crhr2,* and *Pac1r* expression (Figs. 2G, 2I,
312 2K). We observed treatment [F(1,25)=33.72, P<0.0001] and exposure [F(1,25)=9.377, P=0.0052]
313 effects, as well as an interaction [F(1,25)=13.02, P=0.0013] effect in *Crhr1* expression with an
314 increase in OPFR control males compared to OPFR restrained (~2-fold; P<0.001) and oil control
315 (P<0.0001) males (Fig. 2H). In males, *Pacap* expression was affected by exposure
316 [F(1,24)=4.374, P=0.0473] where there was a decrease in OPFR restrained mice compared to
317 OPFR control mice (P<0.05; Fig. 2J). OPFR treatment increased *Ptpn5* expression in control

318 male mice (P<0.01) with a treatment effect of [F(1,26)=13.47, P=0.0011] (Fig. 2L). Collectively,
319 these findings show that perinatal OPFR exposure alters the expression of central stress-related
320 genes in a sex-dependent manner, particularly affecting *Crhr1*, *Crhr2*, and *Ptpn5* in both control
321 and stressed conditions.
322
323 *OPFR treatment altered pituitary gene expression independent of sex or exposure*
324 We examined CRH-related genes in the pituitary. In females, *Crhr1* expression was affected by
325 treatment [F(1,26)=9.472, P=0.0049] with increased levels in OPFR control females compared to
326 oil control females (P<0.05; Fig. 3A). Treatment effects were more pronounced in male *Crhr1*
327 expression [F(1,24)=36.56, P<0.0001] where both OPFR groups were ~2-fold higher compared
328 to oil groups (P<0.01; P<0.0001; Fig. 3D). *Pomc* (ACTH) expression was affected by treatment
329 in females [F(1,24)=28.70, P<0.0001] and males [F(1,23)=20.37, P=0.0002] where OPFR
330 decreased levels in both exposure groups in both sexes (P<0.01; Fig. 3B and 3E). In females,
331 *Nr3c1* (GR) expression was affected by treatment [F(1,26)=5.406, P=0.0281] and exposure
332 [F(1,26)=6.724, P=0.0154] (Fig. 3C). In males, *Nr3c1* expression was affected by treatment
333 [F(1,24)=23.60, P<0.0001] where OPFR increased expression in both exposure groups (P<0.01;
334 Fig. 3F). These data indicate that OPFR treatment disrupts pituitary expression of key stress-axis
335 genes, including *Crhr1*, *Pomc*, and *Nr3c1*, in both males and females, independent of stress
336 exposure.
337
338 *Perinatal OPFR treatment led to blunted adrenal gene expression in female offspring*
339 Genes along the catecholamine pathway in the adrenals from adult offspring were analyzed. In
340 females, *Dbh* expression was affected by treatment [F(1,23)=11.01, P=0.0030] and exposure

341 [F(1,23)=6.619, P=0.0170] with a ~2-fold decrease in the oil restrained group compared to oil
342 control and OPFR restrained group (P<0.01; Fig. 4A). *Pnmt* expression was affected by
343 treatment [F(1,24)=22.39, P<0.0001] and exposure [F(1,24)=4.881, P=0.0370] with an increase
344 in oil restrained females compared to oil control (P<0.05) and OPFR restrained (P<0.001)
345 females (Fig. 4B). In addition, OPFR treatment decreased *Pnmt* expression in control females
346 (P<0.05). No differences were seen for male *Dbh* expression (Fig. 4C). In males, *Pnmt*
347 expression was affected by exposure [F(1,24)=6.194, P=0.0202] with an increase in oil restrained
348 mice compared to oil control mice (P<0.01; Fig. 4D).
349 The steroidogenic pathway (Fig. S1) was analyzed in adrenals collected from adult
350 offspring. In females, an exposure effect was noted for *Mc2r* expression [F(1,24)=5.793,
351 P=0.0241] with a decrease in the oil restrained group compared to oil control group (P<0.01; Fig.
352 S1A). No differences were found for the following genes in females: *Cyp11a1*, *Cyp21a1*, and
353 *Cyp11b1* (Figs. S1B-1D). In females, *Cyp11b2* expression was lower in OPFR control mice
354 compared to oil control mice (P<0.05; Fig. S1E). In males, no differences in expression were
355 observed for steroidogenic genes: *Mc2r*, *Cyp11a1*, *Cyp21a1*, *Cyp11b1,* or *Cyp11b2* (Figs. S1F-
356 1J). These data provide evidence that OPFR exposure and stress affect adrenal gene expression
357 in females more than males, especially in genes related to catecholamine biosynthesis (*Dbh*,
358 *Pnmt*), while steroidogenic gene expression was largely unaltered in males.
359
360 *AVS exposure affected HPA axis response in OPFR-treated female offspring*
361 CORT analysis revealed an effect of exposure [F(1,28)=6.082, P=0.0200] where OPFR AVS
362 females had decreased levels compared to OPFR control females (P<0.05) (Fig. 5A). There was
363 also a trending increase (P=0.0581) in CORT serum in OPFR control females compared to oil

364 control females which could account for the significant difference within the OPFR group. No
365 effects were seen for CORT levels in males (Fig. 5B). Overall, OPFR-treated females exhibited
366 altered HPA axis responsivity, with decreased corticosterone after AVS, while male
367 corticosterone levels remained unaffected.
368
369 *Perinatal OPFR treatment has a greater impact on PVN gene expression than AVS exposure*
370 We selected genes that are part of the central stress response pathway and a marker of
371 inflammation. In females, no effects were seen for *Crh* or *Crhr2* expression (Fig. S2A and S2B).
372 A treatment effect was seen for *Crhr1* expression in females [F(1,19)=8.095, P=0.0103], with a
373 decrease in OPFR control group compared to oil control group (P<0.05; Fig. 6A). Treatment
374 effects were seen in female *Pacap* and *Pac1r* expression [F(1,19)=27.44, P<0.0001;
375 F(1,19)=28.03, P<0.0001], with a ~2-fold increase in OPFR groups compared to oil groups for
376 both genes (P<0.01; Fig. 6B and 6C). *Ikk,* a regulator of the inflammatory NF-kB pathway, was
377 affected by exposure [F(1,17)=10.04, P=0.0056], including an increase in oil AVS females
378 compared to oil control females (P<0.05; Fig. S2C). No effects were seen in *Ptpn5* expression
379 for females or males (not shown).
380 In males, no effects were seen in *Crh, Crhr2,* or *Ikk* expression (Figs. S2D-S2F). We
381 observed a treatment effect for *Crhr1* expression [F(1,19)=15.20, P=0.0010] with a decrease in
382 OPFR AVS males compared to oil AVS males (P<0.001; Fig. 6D). Similar to females, treatment
383 effects were seen in male *Pacap* and *Pac1r* expression [F(1,20)=37.51, P<0.0001;
384 F(1,20)=43.39, P<0.0001], with a ~2-fold increase in OPFR groups compared to oil groups for
385 both genes (P<0.001; Fig. 6E and 6F). Collectively, these findings show that perinatal OPFR

386 treatment alters expression of stress-related and inflammatory genes in the PVN, with increased
387 *Pacap* pathway expression in both sexes and sex-specific effects on *Crhr1* and *Ikk*.
388
389 *Perinatal OPFR treatment and AVS exposure disrupted PACAP pathway in the BNST of female*
390 *offspring*
391 We also investigated the expression of stress-related genes in the adBNST since GABAergic
392 projections from the adBNST to the PVN are involved in negative feedback of the HPA axis
393 (31). In females, no differences were seen in *Crh* or *Crhr2* (Fig. S3A and S3B). *Crhr1* expression
394 was affected by treatment [$F(1,24)=4.835$, $P=0.0378$] where OPFR control females had increased
395 levels compared to oil control females ($P<0.05$; Fig. 7A). We observed treatment, exposure, and
396 interaction effects in female *Pacap* expression [$F(1,25)=4.381$, $P=0.0467$; $F(1,25)=50.20$,
397 $P<0.0001$; $F(1,25)=5.899$, $P=0.0227$], where OPFR treatment increased expression by ~3-fold
398 ($P<0.01$) and AVS decreased expression within the OPFR group ($P<0.01$; Fig. 7B). *Pac1r*
399 expression was affected by treatment [$F(1,24)=177.1$, $P<0.0001$], where OPFR treatment
400 increased expression by ~2.5-fold and AVS decreased expression within the OPFR group
401 ($P<0.05$; Fig. 7C). *Ikk* expression was affected by treatment and exposure [$F(1,25)=5.390$,
402 $P=0.0287$; $F(1,25)=5.636$, $P=0.0256$], with an upregulation in OPFR control and oil AVS females
403 compared to oil control females ($P<0.01$; Fig. S3C).
404 In males, no pairwise differences were seen in *Crh* or *Crhr1* (Fig. S3D and S3E);
405 however, there was a treatment effect for *Crhr1* [$F(1,25)=4.275$, $P=0.0492$]. We observed a
406 decrease in *Crhr2* expression after AVS exposure in OPFR males ($P<0.05$; Fig. 7D). *Pacap* and
407 *Pac1r* expression was affected by treatment [$F(1,24)=55.18$, $P<0.0001$; $F(1,26)=65.17$,
408 $P<0.0001$], where OPFR treatment increased expression by ~3-fold ($P<0.001$; Fig. 7E and 7F).

409 *Ikk* expression was affected by treatment [F(1,26)=87.77, P<0.0001], where OPFR increased
410 overall expression (P<0.0001; Fig. S3F). These data provide evidence that OPFR exposure
411 dysregulates stress and inflammatory signaling in the adBNST in a sex-dependent manner,
412 particularly enhancing *Pacap* pathway and *Ikk* expression, and altering *Crhr1* and *Crhr2*
413 expression.
414
415 *Sex specific response to OFT after OPFR treatment and AVS exposure*
416 The OFT assesses exploratory and avoidant behavior. In females, overall locomotion was not
417 affected (Fig. S4A and S4B). In males, locomotion was affected by AVS exposure, with an
418 increase in distance traveled (F(1,44)=30.00, P<0.0001) and mean speed (F(1,44)=30.51,
419 P<0.0001) regardless of treatment (P<0.01; Fig. S4A and S4B). In females, there was no effects
420 seen for time immobile in the perimeter (Fig. 8A), however there was a significant effect of
421 exposure [F(1,47)=7.185, P=0.0101] where OPFR AVS mice spent a longer time immobile in the
422 corners than OPFR control mice (P<0.05; Fig. 8B). In males, an exposure effect [F(1,44)=6.274,
423 P=0.0160] was noted for time immobile in the perimeter, where OPFR AVS mice spent less time
424 immobile in the perimeter compared to OPFR control mice (P<0.05; Fig. 8C). We also observed
425 effects on treatment [F(1,39)=8.729, P=0.0053] and exposure [F(1,39)=4.416, P=0.0421] for
426 time immobile in the corners, with OPFR AVS mice spending less time immobile than oil AVS
427 mice (P<0.05; Fig. 8D). These findings demonstrate that AVS increases avoidance behavior and
428 alters locomotion in a sex-specific manner, with females showing increased corner behavior and
429 males displaying heightened activity and mobility.
430
431 *AVS increased activity in EPM in control male offspring*

432 The EPM is another test that evaluates avoidance behavior. In males, exposure effects were noted
433 for distance and mean speed [$F(1,45)=7.650$, $P=0.0082$; $F(1,45)=7.594$, $P=0.0084$], where AVS
434 increased the locomotion of oil males ($P<0.05$; Fig. 9E and 9F). Additional exposure effects were
435 observed for closed arms entries and distance traveled [$F(1,45)=7.024$, $P=0.0111$; $F(1,44)=12.96$,
436 $P=0.0008$]. Specifically, AVS increased closed arm entries and distance traveled in oil males, and
437 increased distance traveled of OPFR males ($P<0.05$; Fig. 9G and 9H). Together, these results
438 suggest that AVS enhances avoidance behavior in males, particularly increasing closed-arm
439 activity and overall locomotion in oil- and OPFR-treated mice.
440
441 *Perinatal OPFR treatment and AVS exposure led to sex-specific responses in LDB*
442 The LDB examines exploratory and avoidance behavior. In females, significant effects of
443 exposure were noted for light zone entries and exits [$F(1,45)=7.351$, $P=0.0095$; $F(1,45)=7.941$,
444 $P=0.0072$], with AVS decreasing both entries and exits in OPFR groups ($P<0.01$; Fig. 10A and
445 10B). The opposite was observed for light zone entries and exits in OPFR males ($P<0.05$; Fig.
446 10E and 10F). In females, exposure effects were noted for dark zone entries and exits
447 [$F(1,46)=4.938$, $P=0.0312$; $F(1,46)=4.359$, $P=0.0424$], with AVS decreasing both entries and
448 exits in OPFR groups ($P<0.05$; Fig. 10C and 10D). In males, exposure effects were also noted for
449 dark zone entries and exits [$F(1,45)=4.103$, $P=0.0488$; $F(1,45)=4.195$, $P=0.0464$]; however, AVS
450 increased entries and exits in OPFR groups ($P<0.05$; Fig. 10G and 10H). These results show that
451 AVS exposure modulates light/dark zone transitions in a sex- and treatment-dependent manner,
452 decreasing exploratory behavior in OPFR females and increasing it in OPFR males.
453
454 *Perinatal OPFR treatment decreases latency to feed in males only*

455 The NSF is a conflict-based test which assesses how long it takes for the mouse to eat the pellet
456 in the center of a brightly lit novel area, with longer latency to eat indicating increased avoidance
457 behavior. In males, we observed an exposure effect for amount of pellet eaten [F(1,39)=9.672,
458 P=0.0035], where oil control males ate more than oil AVS and OPFR control males (P<0.05; Fig.
459 S5D). Latency to eat in the novel arena was affected by treatment [F(1,39)=5.647, P=0.0225],
460 with OPFR decreasing latency in control males (P<0.05; Fig. 11E). The probability to eat as
461 shown by the Kaplan-Meier curve (Fig. 11F), had an effect of treatment in the novel arena where
462 OPFR control males were more likely to eat than oil control males (P= 0.0179). These data
463 suggest that OPFR alters conflict-based avoidance behavior in males, with decreased latency to
464 feed and increased likelihood of eating under anxiogenic conditions.
465

466 **Discussion**

467 While the global use of brominated flame retardants has declined, the use of OPFRs has
468 increased in countries such as the US and China (40). A report from Albany, New York, USA,
469 estimates daily indoor OPFR exposure via inhalation of air, dermal sorption, and dust ingestion
470 at 149, 279, and 390 ng/kg bw/day, respectively (41). Although the combined effects of perinatal
471 OPFR treatment and acute stress have not been studied, *in vitro* evidence has shown that PBDEs
472 increase cortisol and aldosterone production, while TPP decreases their production (26,42). Rat
473 studies using various flame retardants have also shown mixed results, with some reporting
474 increased adrenal weight and CORT levels (24,26), while others report a dose-dependent
475 decrease in adrenal weight and CORT in males only (23). Human data have linked increased
476 OPE diester concentrations with 18%-41% higher cortisol and cortisone levels (43). In our study,
477 we observed sex-dependent disruption of the HPA axis by perinatal OPFR treatment.

478 Both females and males demonstrated exposure effects for CORT levels that were
479 elevated after 1 h restraint. However, only OPFR-treated females exhibited a significant increase
480 in CORT, while oil-treated females did not. This suggests that perinatal OPFR treatment may
481 exacerbate stress response in females. Electrophysiological recordings have shown that treatment
482 with 17β-estradiol (E2) increase PVN CRH neuronal activity and correlate with CORT levels,
483 therefore it is possible that OPFR treatment is eliciting similar effects to endogenous hormones
484 (44). The higher variability in CORT levels among oil control females, coupled with a slightly
485 lower (though not significant) average in OPFR controls, may contribute to this treatment-
486 specific difference. Previous studies have shown that female rodents have more pronounced
487 stress responses than males which may also account for these effects (45,46). Sex differences in
488 CORT levels have also been noted in humans, where women with depression have been reported
489 to have higher cortisol levels than non-depressed women (47). No differences were noted for
490 epinephrine levels between groups, likely because levels had returned to baseline after 1 h of
491 restraint. Previous work in male mice shows epinephrine peaking at ~40 minutes post-stress (48),
492 which aligns with this finding.
493 In the PVN, an exposure effect was noted for *Crh* and *Crh2* in females, with there being a
494 significant increase in *Crhr2* following stress in the OPFR group. CRH R2 is important for
495 ACTH production and recovery of the HPA axis recovery, as previously shown in *Crhr2*
496 knockout mice (49). This response may be exacerbated in OPFR-treated females due to trending
497 decrease in OPFR-control expression of *Crhr2*. We also observed a treatment-related decrease in
498 *Pac1r*, which encodes a receptor for PACAP, a neuropeptide that activates CRH neurons and
499 stimulates the stress axis (50). The observed increase in *Crhr2* and decrease in *Pac1r* may reflect
500 HPA axis recovery processes occurring during the restraint period, which aligns with prior

501 reports showing CORT peaking 30–60 minutes into restraint and recovery initiating while the
502 stressor remains present (51). In females and males, increased *Ptpn5* expression in OPFR control
503 mice suggests long-term effects on synaptic plasticity in the PVN resulting from perinatal OPFR
504 exposure.

505 In males, we saw pronounced differences in *Crhr1* expression, with elevated levels in
506 OPFR-control animals compared to both oil control males and OPFR-restrained males. While no
507 EDC studies have previously reported increased *Crhr1* expression in the PVN, one study of
508 gestational intermittent hypoxia (GIH) found increased protein levels of CRHR1 in the PVN of
509 embryonic day (E) 19 male mice, but not female mice (52). Interestingly, they associated GIH
510 reprogramming of CRH R1 signaling in the PVN to anxiogenic effects in adult rat offspring. Our
511 previous work found anxiogenic effects of perinatal OPFR treatment in the open field test and
512 anxiolytic effects in the elevated plus maze in unrestrained male offspring (36). The elevated
513 *Crhr1* expression observed here may reflect fetal programming that sensitizes the pituitary to
514 CRH. Decreases in both *Crhr1* and *Pacap* in OPFR-restrained males may indicate negative
515 feedback mechanisms within the central stress response pathway.

516 In the pituitary, significant treatment effects were observed in females and males across
517 all genes analyzed. Perinatal OPFR treatment increased *Crhr1* expression but decreased *Pomc*
518 expression, likely due to elevated *Nr3c1* (GR) expression, which negatively regulates *Pomc*. GRs
519 are activated by high CORT levels and partake in the negative feedback loop that terminates the
520 stress response (53). They are known targets of EDCs, including flame retardants (20,54-56). A
521 developmental study conducted in zebrafish larvae showed dose-dependent increases in GR
522 mRNA expression following TDCPP and TPP treatment (57). In our study, *Nr3c1* expression was
523 affected by both treatment and exposure in females, while treatment effects were more prominent

524 in males with pairwise differences. These increases in *Nr3c1* may alter the regulation of negative
525 feedback in the HPA axis. Future studies could also evaluate GR expression in the hypothalamus,
526 where its role is to reduce *Crh* expression. The OPFR-induced effects in the pituitary were
527 consistent across sexes.

528 In the adrenal glands, no steroidogenic changes were observed in males, whereas a few
529 were found in females. Specifically, *Mc2r* (ACTH receptor) expression decreased in oil
530 restrained females, but not in OPFR-treated counterparts, suggesting that perinatal OPFR
531 treatment may impair adrenal sensitivity to ACTH. Additionally, *Cyp11b2* expression was
532 reduced in OPFR control females, possibly reflecting upstream functional disruptions, as a slight
533 decrease in OPFR control female CORT was also observed. Human adrenal cell studies (H295R,
534 female) have shown increased expression of *Cyp11b1* and *Cyp11b2* following flame retardant
535 exposure (21,22). Although another developmental study using a mixture of EDCs (phthalates,
536 pesticides, and bisphenol A) showed a dose-dependent decrease in *Cyp11b1* adrenal expression
537 in female adult offspring that underwent behavioral testing (58). It is important to note that
538 steroidogenic pathways in rodents differ from humans in that 1) rodents mainly synthesize CORT
539 due to poor Cyp17 expression, 2) rodents utilize HDL cholesterol via the SR-B1 pathway while
540 humans utilize LDL cholesterol via the endocytic pathway as steroid precursors, and 3) mice do
541 not have a zona reticularis and as a result, do not produce androgens (15).

542 Despite the differences between mouse and human adrenal cortices, adrenal medullary
543 function is conserved across both species. During development, neuroendocrine cells from the
544 neural crest invade the adrenal cortex by embryonic day (E) 11 and differentiate into chromaffin
545 cells, completing development by E15 (59). Upon activation of the sympathetic-adrenal-
546 medullary (SAM) axis, these cells release norepinephrine (noradrenaline) and epinephrine

547 (adrenaline), otherwise known as the “fight-or-flight” hormones. These catecholamines enhance
548 cardiovascular output and mobilize energy stores (60). *Dbh* converts dopamine into
549 norepinephrine and *Pnmt* then converts norepinephrine to epinephrine. In females, 1-h restraint
550 decreased *Dbh* expression, but this was blunted by OPFR treatment. Similarly, *Pnmt* expression
551 increased with stress in oil-treated females, but this response was also blunted in OPFR-treated
552 mice. While *Dbh* expression for OPFR-treated and oil control females are at similar levels, *Pnmt*
553 expression of OPFR-treated females fell below that of controls. This could relate to slightly
554 reduced serum CORT levels in OPFR females, as CORT regulates PNMT activity. These
555 treatment-related changes in females likely stem from disrupted embryonic development of the
556 adrenal medulla. In males, we observed increased *Pnmt* following stress, as expected, though the
557 response was blunted in OPFR-treated males, although not statistically significant. These
558 patterns suggest medullary development may also be impacted in males, though to a lesser
559 degree.

560 Utilizing a 6-day AVS paradigm, we revealed that perinatal OPFR treatment can lead to
561 deficits in central stress response and behavior in adulthood. In OPFR AVS females, we observed
562 blunted levels of CORT, BNST *Pacap* and *Pac1r* mRNA expression, as well as increased
563 avoidance and immobility suggesting a weakened HPA axis response. In males, we saw that
564 overall perinatal OPFR treatment increased *Pacap*, *Pac1r*, and *Ikk* in the BNST. For male
565 behavior, AVS increased avoidance while OFPR increased hyperactivity. Overall, our study
566 demonstrated striking sex differences in response to adult acute stress after perinatal OPFR
567 treatment.

568 For CORT levels, we observed sex-specific vulnerability, with OPFR AVS females
569 showing reduced CORT. Additionally, there was a trending increase in CORT in OPFR control

570 females relative to oil controls, which is driving this exposure effect. Other studies have also
571 reported elevated CORT following prenatal EDC treatment (61). It is important to note that these
572 samples were collected 5 days after the last stressor, during the morning when CORT levels are
573 lowest in rodents. Future studies may therefore benefit from measuring CORT immediately after
574 the last stressor through submandibular bleeds to determine immediate effects on the stress
575 response. Especially since other studies have typically seen increases in CORT in females after
576 acute stress paradigms (30).

577 For the neural stress circuitry, treatment differences were noted in both females and
578 males, especially with *Pacap* and its receptor. We saw ~2-fold increases in the PVN and ~3-fold
579 increases in the BNST after OPFR treatment which shows excitability of PACAP pathways in the
580 central stress response. The upregulation in this pathway indicates increased avoidance, which
581 was noted in both groups for behavior. PACAP-deficient mice have demonstrated attenuation of
582 stress-induced responses, including diminished CORT release and reduced activation of the HPA
583 axis (62,63). This further supports the idea that PACAP is crucial for promoting the stress
584 response. Interestingly, we observed a decrease in *Pacap* and its receptor after AVS exposure in
585 OPFR-treated females. This reduction is consistent with the observed decrease in CORT levels in
586 females and aligns with existing literature linking PACAP signaling to HPA axis regulation (50).
587 Notably, this exposure-related change was not observed in males within the BNST, supporting
588 both our previous findings and other research demonstrating BNST sex-specific response to
589 stress (34,64).

590 Perinatal OPFR treatment also led to increases in the inflammatory mediator *Ikk*, a key
591 component of the NF-κB pathway. Specifically, we observed elevated *Ikk* expression in oil AVS
592 females in both the PVN and BNST, aligning with existing literature that highlights the role of

593 proinflammatory mediators in the stress response, particularly following chronic restraint stress
594 (65). Importantly, we did not observe these exposure-related increases in Ikk in males,
595 suggesting a sexually dimorphic stress response which has previously documented in other 6-day
596 stress models, where female mice show greater susceptibility to depression-like behaviors
597 (30,66). Interestingly, we saw significant treatment differences on *Ikk* in males and females only
598 in the BNST. OPFRs are known to induce neurotoxicity through inflammatory pathways (67-70).
599 In addition, NHANES epidemiologic data have demonstrated a significant positive association
600 between urinary OPFR concentrations, elevated inflammatory markers, and the risk of
601 depression in humans (12). An additional mouse model of *in utero* OPFR exposure also
602 demonstrated placenta inflammation, disrupted neuronal development and synaptic transmission,
603 and persistent avoidant behaviors in adulthood (71). Together, these findings suggest that early-
604 life OPFR exposure may produce long-lasting neurobehavioral effects by promoting persistent
605 inflammation. More inflammatory markers further down the Ikk pathway, such as IL-1, should
606 be explored in future studies to elucidate this mechanism of OPFR-induced neurotoxicity.
607 The behavior tests that were conducted demonstrated pronounced sex-specific effects in
608 response to perinatal OPFR treatment and AVS exposure. In the OFT, OPFR AVS females had
609 increased immobility in the corners, indicative of increased avoidant behavior. This may be due
610 to hypoactivation of the HPA axis, although more measurements of CORT levels would need to
611 be taken immediately after stressors to confirm. For males, we saw an increase in locomotion
612 and corner time after AVS. Perinatal OPFR treatment induced hyperactivity, as we also observed
613 a trending increase in time mobile in OPFR AVS males. The combined effects of OPFR and AVS
614 made males more hyperactive in the perimeter, noted by reduced immobility in the perimeter and

615 corners and pattern of movement in the heat maps. We have previously also seen that perinatal
616 OPFR treatment leads to hyperactivity in males (36).

617 In the EPM, males showed increased locomotion, closed arm entries and distance after
618 AVS, confirming hyperactivity and avoidance seen in OFT. In the LDB, OPFR AVS females had
619 reduced dark and light entries/exits whereas OPFR AVS males had the opposite effect. Male
620 OPFR controls had a trending decreasing in distance traveled in the light zone demonstrating
621 avoidance, however AVS abolished this effect to levels comparable to oil AVS males. In the NSF,
622 we saw treatment differences where OPFR males had reduced latency to eat, reflecting reduced
623 avoidance. AVS exposure eliminated this treatment difference, supporting previous tests of
624 increased avoidance in OPFR AVS groups.

625 Overall, the behavior tests indicate that OPFR AVS females display increased avoidance
626 and reduced activity. Increased immobility may reflect a passive reaction coping mechanism,
627 often associated with depressive-like behavior, and similar increases in immobility have been
628 observed in females exposed to a low-dose mixture of EDCs (61). Therefore, future studies
629 should investigate whether perinatal OPFR treatment combined with AVS exposure affects
630 motivation-related behaviors, particularly given that the BNST is implicated in effort-based
631 decision and motivation behaviors (72). Future work could determine whether OPFR treatment
632 and AVS exposure increase freezing behavior. During the final stressor, which involved acoustic
633 stimuli from a startle box, no group differences were found in startle amplitude. However,
634 treatment- and sex-specific differences emerged during the “null periods” between stimuli:
635 OPFR females exhibited delayed movement following stimulus cessation compared to oil
636 females and OPFR males. These findings highlight a potential sex-specific vulnerability to
637 OPFR and AVS exposure, suggesting that OPFR-treated females may exhibit heightened

638 behavioral inhibition and altered stress response due to HPA dysregulation. It is possible that
639 perinatal OPFR treatment alters glucocorticoid or mineralocorticoid related feedback
640 mechanisms which may account for these differences (28,31).
641
642 **Conclusion**
643 This study demonstrates that perinatal exposure to organophosphate flame retardants (OPFRs)
644 leads to long-lasting, sex-specific disruptions in the neuroendocrine stress response. Female
645 OPFR-treated offspring exhibited heightened corticosterone release following restraint stress.
646 These changes were accompanied by significant modulation of gene expression in the
647 paraventricular nucleus (PVN), pituitary, and adrenal glands, particularly in genes involved in
648 CRH signaling, glucocorticoid feedback, and catecholamine synthesis. The lower basal CORT
649 levels in OPFR AVS females points to dysregulation of mechanisms within the HPA axis. These
650 effects were particularly pronounced in stress-sensitive brain regions such as the BNST and
651 PVN, further supporting a sex-dependent vulnerability. Given that OPFRs interfere with
652 hormone receptor function, these findings may implicate disrupted receptor-mediated signaling
653 during critical periods of brain development. Collectively, these results provide compelling
654 evidence that early-life OPFR treatment reprograms central stress circuits, with long-lasting
655 consequences on behavioral and endocrine responses to stress. These alterations may increase
656 susceptibility to mood and anxiety disorders, particularly in females, underscoring the need for
657 further investigation into sex-specific mechanisms and long-term neurobehavioral outcomes.
658
659

Author Contributions: Conceptualization, T.A.R, C.M.R; investigation, C.M.R, A.Y, C.B, J.D, S.C; analysis, C.M.R, N.B; resources, T.A.R, N.B; writing-original draft preparation, C.M.R; writing- review and editing, C.M.R, T.A.R, N.B; supervision, T.A.R; funding acquisition, T.A.R.

Funding: This research was supported by funds from National Institutes of Health (R01MH123544; R21ES035848; P30ES005022). C.M.R. was previously supported by and C.B. is currently supported by the National Institute of Environmental Health Sciences (T32ES007148).

Disclosures: The authors have nothing to disclose.

Data Availability: The data that support the findings of this study are available in the Materials and Methods and/or Results section of this article. Supplementary Materials are available at (editor will insert link??)

References

1. de Boer J, Harrad S, Sharkey M. The European Regulatory Strategy for flame retardants–The right direction but still a risk of getting lost. *Chemosphere*. 2024;347:140638.
2. Blum A, Behl M, Birnbaum LS, et al. Organophosphate ester flame retardants: are they a regrettable substitution for polybrominated diphenyl ethers? *Environmental Science & Technology Letters*. 2019;6(11):638-649.
3. van Melis LVJ, Zimnik KN, Persad AR, et al. Exposure to organophosphate flame retardants and phthalates alters neuronal activity and network development. *Toxicology*. Aug 2025;515:154168. doi:10.1016/j.tox.2025.154168
4. Yan Z, Feng C, Jin X, et al. Organophosphate esters cause thyroid dysfunction via multiple signaling pathways in zebrafish brain. *Environ Sci Ecotechnol*. Oct 2022;12:100198. doi:10.1016/j.ese.2022.100198
5. Percy Z, Vuong AM, Xu Y, et al. Maternal Urinary Organophosphate Esters and Alterations in Maternal and Neonatal Thyroid Hormones. *American Journal of Epidemiology*. 2021;190(9):1793-1802. doi:10.1093/aje/kwab086
6. Li Y, Zhao M, Shen X, et al. Adverse Effects of Aryl Organophosphate Esters on Reproduction. *Environ Sci Technol*. Jun 3 2025;59(21):10122-10135. doi:10.1021/acs.est.5c01992
7. Van den Eede N, Dirtu AC, Neels H, Covaci A. Analytical developments and preliminary assessment of human exposure to organophosphate flame retardants from indoor dust. *Environ Int*. Feb 2011;37(2):454-61. doi:10.1016/j.envint.2010.11.010
8. Butt CM, Congleton J, Hoffman K, Fang M, Stapleton HM. Metabolites of organophosphate flame retardants and 2-ethylhexyl tetrabromobenzoate in urine from paired mothers and toddlers. *Environ Sci Technol*. Sep 2 2014;48(17):10432-8. doi:10.1021/es5025299
9. Doherty BT, Hoffman K, Keil AP, et al. Prenatal exposure to organophosphate esters and behavioral development in young children in the Pregnancy, Infection, and Nutrition Study. *Neurotoxicology*. 2019;73:150-160.
10. Dubovický M. Neurobehavioral manifestations of developmental impairment of the brain. *Interdiscip Toxicol*. Jun 2010;3(2):59-67. doi:10.2478/v10102-010-0012-4
11. Rojas CM, Wiersielis KR, Roepke TA. Mechanisms of Flame Retardant Toxicity and Their Impacts on Anxiety and Cognition in the Brain. *Endocrinology*. Apr 15 2025;doi:10.1210/endocr/bqaf074
12. Chen Y-X, Zheng J, Zhang X-F. Association analysis between organophosphorus flame retardants exposure and the risk of depression: Data from NHANES 2017–2018. *Journal of Affective Disorders*. 2024/06/15/ 2024;355:385-391. doi:https://doi.org/10.1016/j.jad.2024.04.004
13. Lu M, Han F, Liu Y, et al. Pregnancy-related anxiety modifies the effects of maternal exposure to organophosphate esters on preschoolers' behavioral development. *Environmental Research*. 2025/04/15/ 2025;271:121081. doi:https://doi.org/10.1016/j.envres.2025.121081
14. Panagiotakopoulos L, Neigh GN. Development of the HPA axis: where and when do sex differences manifest? *Front Neuroendocrinol*. Aug 2014;35(3):285-302. doi:10.1016/j.yfrne.2014.03.002

15. Shen W-J, Azhar S, Kraemer FB. ACTH Regulation of Adrenal SR-B1. Review. *Frontiers in Endocrinology*. 2016-May-13 2016;Volume 7 - 2016doi:10.3389/fendo.2016.00042
16. Bhagavan NV, Ha C-E. Chapter 30 - Endocrine Metabolism III: Adrenal Glands. In: Bhagavan NV, Ha C-E, eds. *Essentials of Medical Biochemistry (Second Edition)*. Academic Press; 2015:559-575.
17. Osinga TE, van den Eijnden MHA, Kema IP, et al. Unilateral and Bilateral Adrenalectomy for Pheochromocytoma Requires Adjustment of Urinary and Plasma Metanephrine Reference Ranges. *The Journal of Clinical Endocrinology & Metabolism*. 2013;98(3):1076-1083. doi:10.1210/jc.2012-3418
18. Sawchenko PE, Arias C. Evidence for Short-Loop Feedback Effects of ACTH on CRF and Vasopressin Expression in Parvocellular Neurosecretory Neurons. *Journal of Neuroendocrinology*. 1995;7(9):721-731. doi:https://doi.org/10.1111/j.1365-2826.1995.tb00814.x
19. Harris AP, Holmes MC, de Kloet ER, Chapman KE, Seckl JR. Mineralocorticoid and glucocorticoid receptor balance in control of HPA axis and behaviour. *Psychoneuroendocrinology*. May 2013;38(5):648-58. doi:10.1016/j.psyneuen.2012.08.007
20. Zhang Q, Wang J, Zhu J, Liu J, Zhao M. Potential Glucocorticoid and Mineralocorticoid Effects of Nine Organophosphate Flame Retardants. *Environmental Science & Technology*. 2017/05/16 2017;51(10):5803-5810. doi:10.1021/acs.est.7b01237
21. Zhang Q, Yu C, Fu L, Gu S, Wang C. New Insights in the Endocrine Disrupting Effects of Three Primary Metabolites of Organophosphate Flame Retardants. *Environmental Science & Technology*. 2020/04/07 2020;54(7):4465-4474. doi:10.1021/acs.est.9b07874
22. Li Z, Robaire B, Hales BF. The Organophosphate Esters Used as Flame Retardants and Plasticizers Affect H295R Adrenal Cell Phenotypes and Functions. *Endocrinology*. Aug 1 2023;164(9)doi:10.1210/endocr/bqad119
23. Li Z, Hales BF, Robaire B. Impact of exposure to a mixture of organophosphate esters on the adrenal glands of Sprague Dawley rats. *Toxicological Sciences*. 2024;204(1):43-56. doi:10.1093/toxsci/kfae154
24. Wade MG, Kawata A, Rigden M, Caldwell D, Holloway AC. Toxicity of Flame Retardant Isopropylated Triphenyl Phosphate: Liver, Adrenal, and Metabolic Effects. *Int J Toxicol*. Jul/Aug 2019;38(4):279-290. doi:10.1177/1091581819851502
25. Akimoto T, Kobayashi S, Nakayama A, et al. Toxicological effects of Tris (1,3-dichloro-2-propyl) phosphate exposure in adult male rats differ depending on the history of exposure in the neonatal period. *J Appl Toxicol*. Sep 2022;42(9):1503-1509. doi:10.1002/jat.4316
26. Dungar BM, Schupbach CD, Jacobson JR, Kopf PG. Adrenal Corticosteroid Perturbation by the Endocrine Disruptor BDE-47 in a Human Adrenocortical Cell Line and Male Rats. *Endocrinology*. 2021;162(11)doi:10.1210/endocr/bqab160
27. Chrousos GP, Gold PW. The concepts of stress and stress system disorders: overview of physical and behavioral homeostasis. *Jama*. 1992;267(9):1244-1252.
28. Handa RJ, Weiser MJ. Gonadal steroid hormones and the hypothalamo-pituitary-adrenal axis. *Front Neuroendocrinol*. Apr 2014;35(2):197-220. doi:10.1016/j.yfrne.2013.11.001
29. Gong S, Miao Y-L, Jiao G-Z, et al. Dynamics and Correlation of Serum Cortisol and Corticosterone under Different Physiological or Stressful Conditions in Mice. *PLOS ONE*. 2015;10(2):e0117503. doi:10.1371/journal.pone.0117503

30. Hodes GE, Pfau ML, Purushothaman I, et al. Sex Differences in Nucleus Accumbens Transcriptome Profiles Associated with Susceptibility versus Resilience to Subchronic Variable Stress. *J Neurosci*. Dec 16 2015;35(50):16362-76. doi:10.1523/jneurosci.1392-15.2015

31. Lebow MA, Chen A. Overshadowed by the amygdala: the bed nucleus of the stria terminalis emerges as key to psychiatric disorders. *Molecular Psychiatry*. 2016/04/01 2016;21(4):450-463. doi:10.1038/mp.2016.1

32. Degroat TJ, Paladino SE, Denney K, Moran KM, Samuels BA, Roepke TA. Chronic social instability stress differentially affects the behavior and the transcriptome of the anterodorsal bed nucleus of the stria terminalis between male and female mice. *bioRxiv*. Jan 21 2025;doi:10.1101/2025.01.21.634142

33. Degroat TJ, Paladino SE, Samuels BA, Roepke TA. Chronic variable mild stress alters the transcriptome and signaling properties of the anterodorsal bed nucleus of the stria terminalis in a sex-dependent manner. *J Neuroendocrinol*. Aug 2025;37(8):e70041. doi:10.1111/jne.70041

34. Degroat TJ, Wiersielis K, Denney K, et al. Chronic stress and its effects on behavior, RNA expression of the bed nucleus of the stria terminalis, and the M-current of NPY neurons. *Psychoneuroendocrinology*. 2024/03/01/ 2024;161:106920. doi:https://doi.org/10.1016/j.psyneuen.2023.106920

35. Adams S, Wiersielis K, Yasrebi A, et al. Sex- and age-dependent effects of maternal organophosphate flame-retardant exposure on neonatal hypothalamic and hepatic gene expression. *Reprod Toxicol*. Jun 2020;94:65-74. doi:10.1016/j.reprotox.2020.04.001

36. Wiersielis KR, Adams S, Yasrebi A, Conde K, Roepke TA. Maternal exposure to organophosphate flame retardants alters locomotor and anxiety-like behavior in male and female adult offspring. *Horm Behav*. Jun 2020;122:104759. doi:10.1016/j.yhbeh.2020.104759

37. Daldrup T, Remmes J, Lesting J, et al. Expression of freezing and fear-potentiated startle during sustained fear in mice. *Genes, Brain and Behavior*. 2015;14(3):281-291. doi:https://doi.org/10.1111/gbb.12211

38. Koenig JI, Elmer GI, Shepard PD, et al. Prenatal exposure to a repeated variable stress paradigm elicits behavioral and neuroendocrinological changes in the adult offspring: potential relevance to schizophrenia. *Behav Brain Res*. Jan 30 2005;156(2):251-61. doi:10.1016/j.bbr.2004.05.030

39. Krumm EA, Patel VJ, Tillery TS, et al. Organophosphate flame-retardants alter adult mouse homeostasis and gene expression in a sex-dependent manner potentially through interactions with ERα. *Toxicological sciences*. 2018;162(1):212-224.

40. Shi S, Feng Q, Zhang J, et al. Global patterns of human exposure to flame retardants indoors. *Science of The Total Environment*. 2024/02/20/ 2024;912:169393. doi:https://doi.org/10.1016/j.scitotenv.2023.169393

41. Kim U-J, Wang Y, Li W, Kannan K. Occurrence of and human exposure to organophosphate flame retardants/plasticizers in indoor air and dust from various microenvironments in the United States. *Environment International*. 2019/04/01/ 2019;125:342-349. doi:https://doi.org/10.1016/j.envint.2019.01.065

42. Li Y, Wang X, Zhu Q, et al. Organophosphate Flame Retardants in Pregnant Women: Sources, Occurrence, and Potential Risks to Pregnancy Outcomes. *Environmental Science & Technology*. 2023/05/09 2023;57(18):7109-7128. doi:10.1021/acs.est.2c06503

43. Ji Y, Yao Y, Duan Y, et al. Association between urinary organophosphate flame retardant diesters and steroid hormones: A metabolomic study on type 2 diabetes mellitus cases and controls. *Sci Total Environ*. Feb 20 2021;756:143836. doi:10.1016/j.scitotenv.2020.143836

816 44. Hu P, Liu J, Yasrebi A, et al. Gq Protein-Coupled Membrane-Initiated Estrogen Signaling
817 Rapidly Excites Corticotropin-Releasing Hormone Neurons in the Hypothalamic Paraventricular
818 Nucleus in Female Mice. *Endocrinology*. Sep 2016;157(9):3604-20. doi:10.1210/en.2016-1191
819 45. Rivier C. Gender, sex steroids, corticotropin-releasing factor, nitric oxide, and the HPA
820 response to stress. *Pharmacology biochemistry and behavior*. 1999;64(4):737-751.
821 46. Viau V, Bingham B, Davis J, Lee P, Wong M. Gender and puberty interact on the stress-
822 induced activation of parvocellular neurosecretory neurons and corticotropin-releasing hormone
823 messenger ribonucleic acid expression in the rat. *Endocrinology*. 2005;146(1):137-146.
824 47. Kokras N, Hodes GE, Bangasser DA, Dalla C. Sex differences in the hypothalamic–
825 pituitary–adrenal axis: An obstacle to antidepressant drug development? *British Journal of*
826 *Pharmacology*. 2019;176(21):4090-4106. doi:https://doi.org/10.1111/bph.14710
827 48. Jeong KH, Jacobson L, Pacák K, Widmaier EP, Goldstein DS, Majzoub JA. Impaired
828 basal and restraint-induced epinephrine secretion in corticotropin-releasing hormone-deficient
829 mice. *Endocrinology*. Mar 2000;141(3):1142-50. doi:10.1210/endo.141.3.7370
830 49. Coste SC, Kesterson RA, Heldwein KA, et al. Abnormal adaptations to stress and
831 impaired cardiovascular function in mice lacking corticotropin-releasing hormone receptor-2.
832 *Nat Genet*. Apr 2000;24(4):403-9. doi:10.1038/74255
833 50. Ebner K, Fontebasso V, Ferro F, Singewald N, Hannibal J. PACAP regulates
834 neuroendocrine and behavioral stress responses via CRF-containing neurons of the rat
835 hypothalamic paraventricular nucleus. *Neuropsychopharmacology*. Feb 2025;50(3):519-530.
836 doi:10.1038/s41386-024-02016-9
837 51. Herman JP, McKlveen JM, Ghosal S, et al. Regulation of the Hypothalamic-Pituitary-
838 Adrenocortical Stress Response. *Comprehensive Physiology*. 2016:603-621.
839 52. Fan J-M, Wang X, Hao K, Yuan Y, Chen X-Q, Du J-Z. Upregulation of PVN CRHR1 by
840 gestational intermittent hypoxia selectively triggers a male-specific anxiogenic effect in rat
841 offspring. *Hormones and Behavior*. 2013/01/01/ 2013;63(1):25-31.
842 doi:https://doi.org/10.1016/j.yhbeh.2012.11.005
843 53. Kolber BJ, Wieczorek L, Muglia LJ. Hypothalamic-pituitary-adrenal axis dysregulation
844 and behavioral analysis of mouse mutants with altered glucocorticoid or mineralocorticoid
845 receptor function. *Stress*. Sep 2008;11(5):321-38. doi:10.1080/10253890701821081
846 54. Zhang J, Yang Y, Liu W, Schlenk D, Liu J. Glucocorticoid and mineralocorticoid
847 receptors and corticosteroid homeostasis are potential targets for endocrine-disrupting chemicals.
848 *Environ Int*. Dec 2019;133(Pt A):105133. doi:10.1016/j.envint.2019.105133
849 55. Liu QS, Sun Z, Ren X, et al. Chemical Structure-Related Adipogenic Effects of
850 Tetrabromobisphenol A and Its Analogues on 3T3-L1 Preadipocytes. *Environmental Science &*
851 *Technology*. 2020/05/19 2020;54(10):6262-6271. doi:10.1021/acs.est.0c00624
852 56. Graceli JB, Dettogni RS, Merlo E, et al. The impact of endocrine-disrupting chemical
853 exposure in the mammalian hypothalamic-pituitary axis. *Molecular and Cellular Endocrinology*.
854 2020/12/01/ 2020;518:110997. doi:https://doi.org/10.1016/j.mce.2020.110997
855 57. Liu C, Wang Q, Liang K, et al. Effects of tris(1,3-dichloro-2-propyl) phosphate and
856 triphenyl phosphate on receptor-associated mRNA expression in zebrafish embryos/larvae.
857 *Aquatic Toxicology*. 2013/03/15/ 2013;128-129:147-157.
858 doi:https://doi.org/10.1016/j.aquatox.2012.12.010
859 58. Repouskou A, Papadopoulou A-K, Panagiotidou E, et al. Long term transcriptional and
860 behavioral effects in mice developmentally exposed to a mixture of endocrine disruptors

associated with delayed human neurodevelopment. *Scientific Reports*. 2020/06/09 2020;10(1):9367. doi:10.1038/s41598-020-66379-x

59. Sass B. Embryology, Adrenal Gland, Mouse. In: Jones TC, Capen CC, Mohr U, eds. *Endocrine System*. Springer Berlin Heidelberg; 1996:381-386.

60. Ubuka T. Subchapter 131B - Noradrenaline/adrenaline. In: Ando H, Ukena K, Nagata S, eds. *Handbook of Hormones (Second Edition)*. Academic Press; 2021:1041-1044.

61. Kaimal A, Hooversmith JM, Cherry AD, et al. Prenatal exposure to bisphenol A and/or diethylhexyl phthalate alters stress responses in rat offspring in a sex- and dose-dependent manner. Original Research. *Frontiers in Toxicology*. 2023-December-13 2023;Volume 5 - 2023doi:10.3389/ftox.2023.1264238

62. Stroth N, Eiden LE. Stress hormone synthesis in mouse hypothalamus and adrenal gland triggered by restraint is dependent on pituitary adenylate cyclase-activating polypeptide signaling. *Neuroscience*. Feb 17 2010;165(4):1025-30. doi:10.1016/j.neuroscience.2009.11.023

63. Lehmann ML, Mustafa T, Eiden AM, Herkenham M, Eiden LE. PACAP-deficient mice show attenuated corticosterone secretion and fail to develop depressive behavior during chronic social defeat stress. *Psychoneuroendocrinology*. May 2013;38(5):702-15. doi:10.1016/j.psyneuen.2012.09.006

64. Hammack SE, Braas KM, May V. Chemoarchitecture of the bed nucleus of the stria terminalis: Neurophenotypic diversity and function. *Handb Clin Neurol*. 2021;179:385-402. doi:10.1016/b978-0-12-819975-6.00025-x

65. Wang X, Weng G, Gao Y, Wang Y, Zhang C. Quercetin ameliorates chronic restraint stress- and LPS-induced anxiety-like behaviors by modulating neuroinflammation in the lateral hypothalamus. *Psychopharmacology*. 2025/04/10 2025;doi:10.1007/s00213-025-06784-0

66. Brancato A, Bregman D, Ahn HF, et al. Sub-chronic variable stress induces sex-specific effects on glutamatergic synapses in the nucleus accumbens. *Neuroscience*. May 14 2017;350:180-189. doi:10.1016/j.neuroscience.2017.03.014

67. Liu X, Zhao X, Wang Y, et al. Triphenyl phosphate permeates the blood brain barrier and induces neurotoxicity in mouse brain. *Chemosphere*. 2020/08/01/ 2020;252:126470. doi:https://doi.org/10.1016/j.chemosphere.2020.126470

68. Wang X, Song F. The neurotoxicity of organophosphorus flame retardant tris (1, 3-dichloro-2-propyl) phosphate (TDCPP): main effects and its underlying mechanisms. *Environmental Pollution*. 2024;346:123569.

69. Yun K, Jeon H, Kho Y, Ji K. Potential adverse outcome pathway of neurodevelopmental toxicity, inflammatory response, and oxidative stress induction mediated by three alkyl organophosphate flame retardants in zebrafish larvae. *Chemosphere*. 2024/05/01/ 2024;356:141901. doi:https://doi.org/10.1016/j.chemosphere.2024.141901

70. Zhong X, Wu J, Ke W, et al. Neonatal exposure to organophosphorus flame retardant TDCPP elicits neurotoxicity in mouse hippocampus via microglia-mediated inflammation in vivo and in vitro. *Archives of Toxicology*. 2020/02/01 2020;94(2):541-552. doi:10.1007/s00204-019-02635-y

71. Hong J, Lu X, Wang J, et al. Triphenyl phosphate disturbs placental tryptophan metabolism and induces neurobehavior abnormal in male offspring. *Ecotoxicology and Environmental Safety*. 2022/09/15/ 2022;243:113978. doi:https://doi.org/10.1016/j.ecoenv.2022.113978

72. Maita I, Bazer A, Chae K, et al. Chemogenetic activation of corticotropin-releasing factor-expressing neurons in the anterior bed nucleus of the stria terminalis reduces effortful

motivation behaviors. *Neuropsychopharmacology*. Jan 2024;49(2):377-385. doi:10.1038/s41386-023-01646-9

Figures

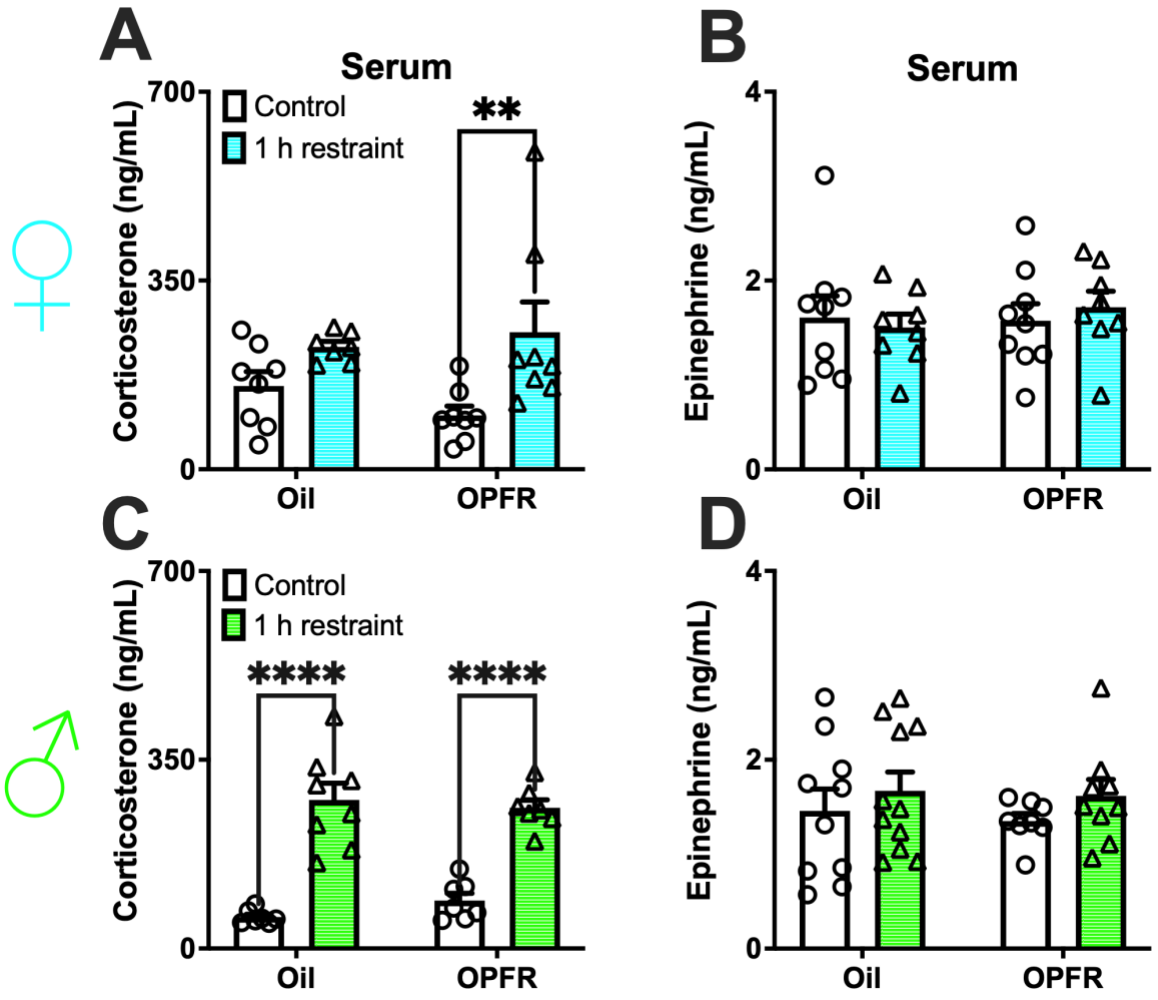

Figure 1. Serum concentrations of corticosterone and epinephrine in (A/B) female and (C/D) male mice. Data are represented as mean ± SEM and dots represent the sample size (number of litters) per treatment and exposure (**= P<0.01, ****= P<0.0001).

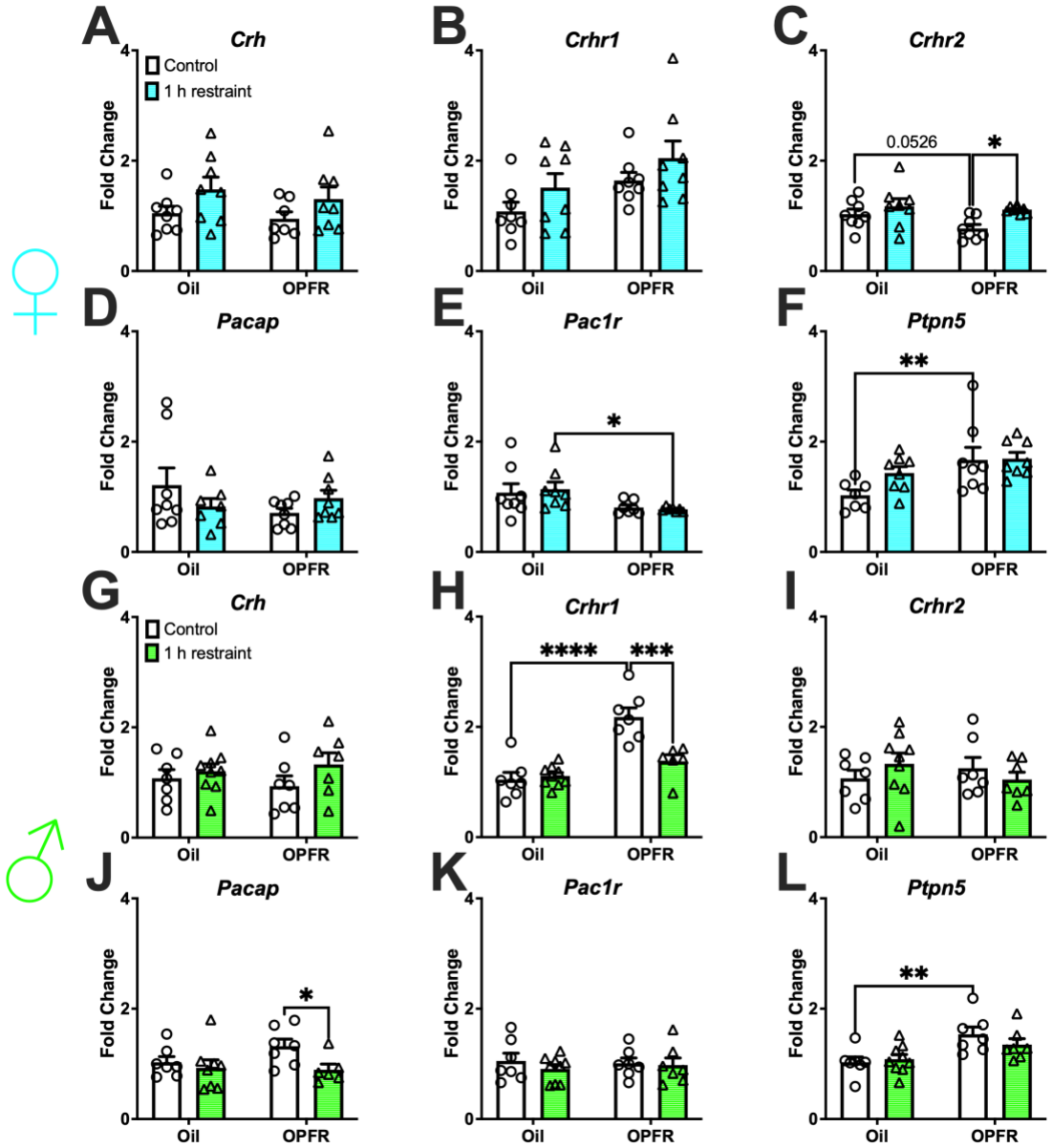

Figure 2. Paraventricular nucleus of the hypothalamus (PVN) mRNA expression in female/male adult offspring. (A/G) *Crh*; (B/H) *Crhr1*; (C/I) *Crhr2*; (D/J) *Pacap*; (E/K) *Pac1r*; and (F/L) *Ptpn5*. Data are represented as mean ± SEM and dots represent the sample size (number of litters) per treatment and exposure. (*= P<0.05, **= P<0.01 , ***= P<0.001, ****= P<0.0001).

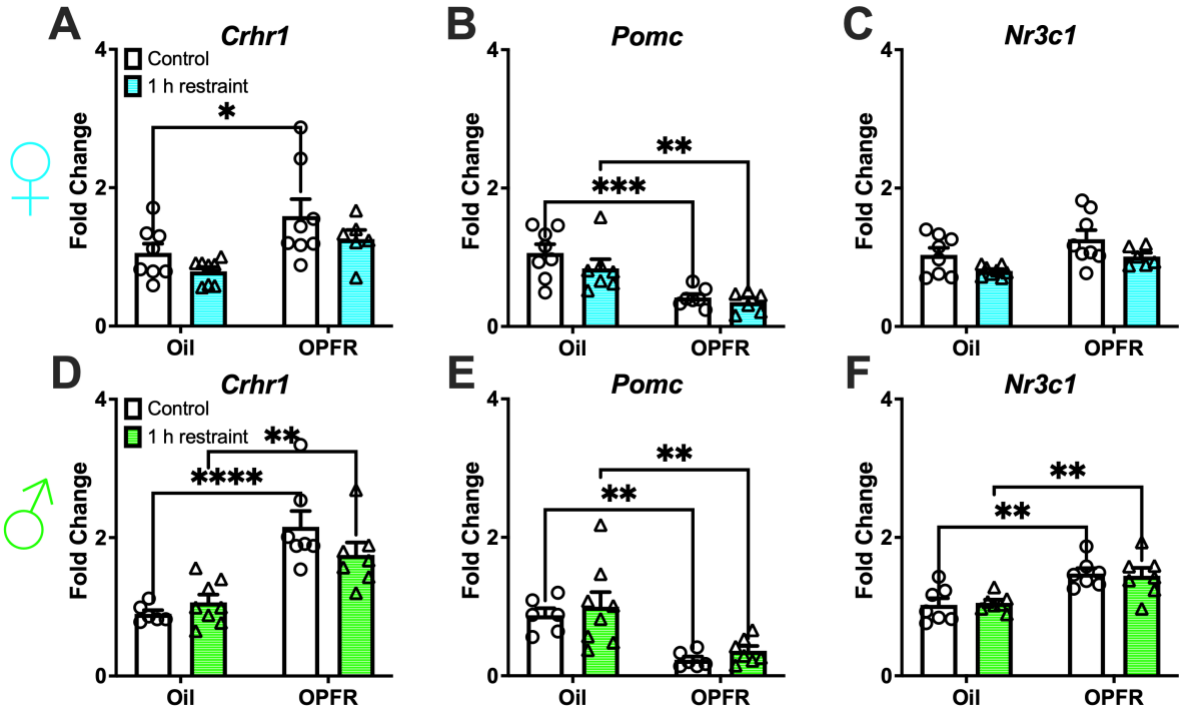

Figure 3. Pituitary mRNA expression in female/male adult offspring: (A/D) *Crhr1*; (B/E) *Pomc*; and (C/F) *Nr3c1*. Data are represented as mean ± SEM and dots represent the sample size (number of litters) per treatment and exposure. (*= P<0.05, **= P<0.01, ***= P<0.001, ****= P<0.0001).

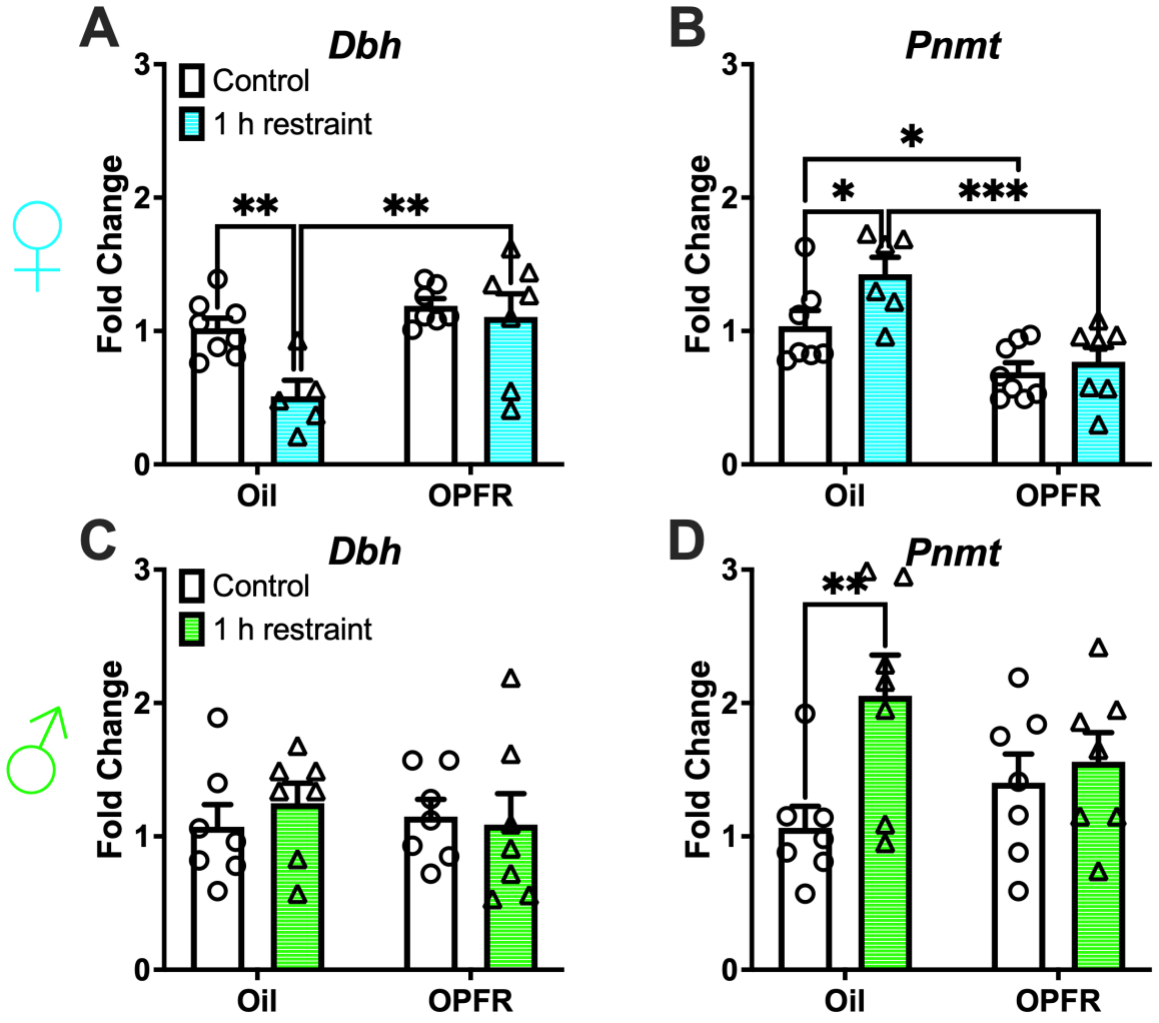

Figure 4. Adrenal mRNA expression of genes in the catecholamine pathway. Female/male adult offspring: (A/C) *Dbh* and (B/D) *Pnmt.* Data are represented as mean ± SEM and dots represent the sample size (number of litters) per treatment and exposure. (*= P<0.05, **= P<0.01, ***= P<0.001).

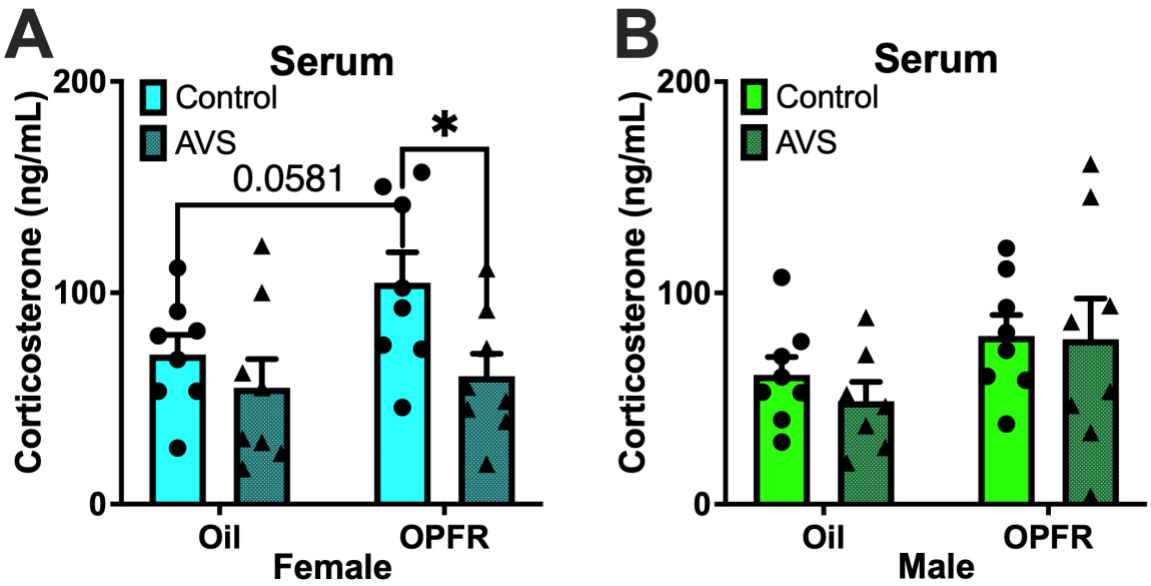

Figure 5. Corticosterone concentrations in serum of (A) female and (B) male mice. Data are represented as mean ± SEM and dots represent the sample size (number of litters) per treatment and exposure (*= P<0.05).

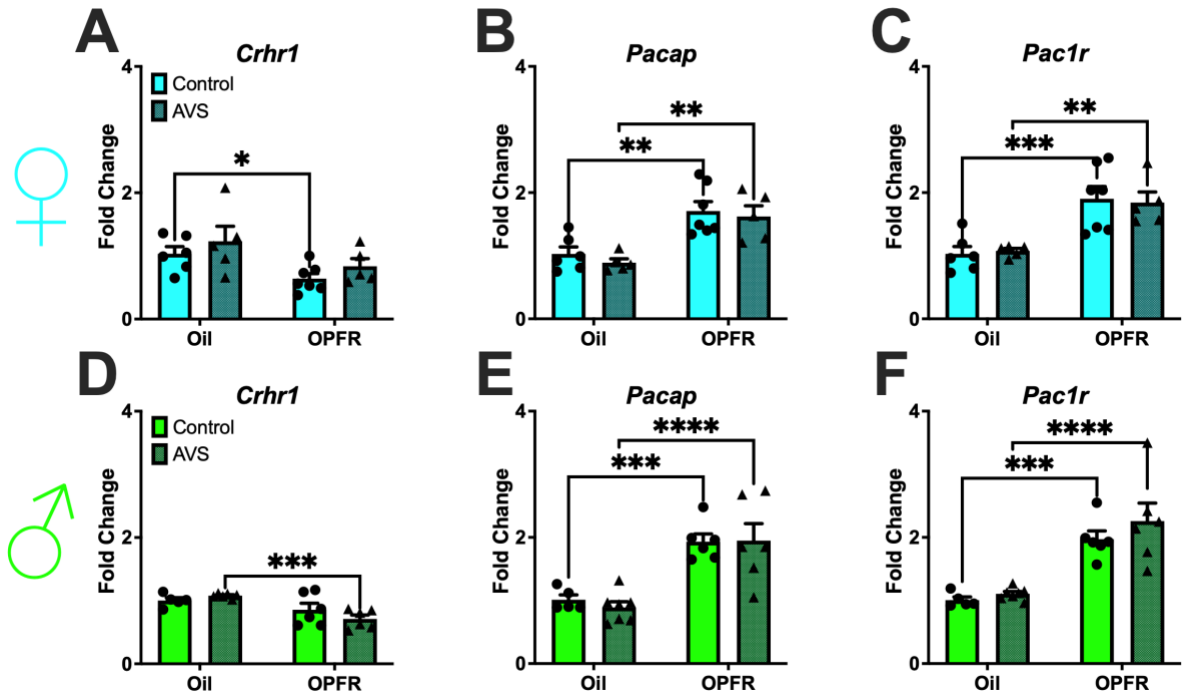

Figure 6. Paraventricular nucleus of the hypothalamus (PVN) mRNA expression in female/male adult offspring. (A/D) *Crhr1*; (B/E) *Pacap*; and (C/F) *Pac1r*. Data are represented as mean ± SEM and dots represent the sample size (number of litters) per treatment and exposure. (*= P<0.05, **= P<0.01, ***= P<0.001, ****= P<0.0001).

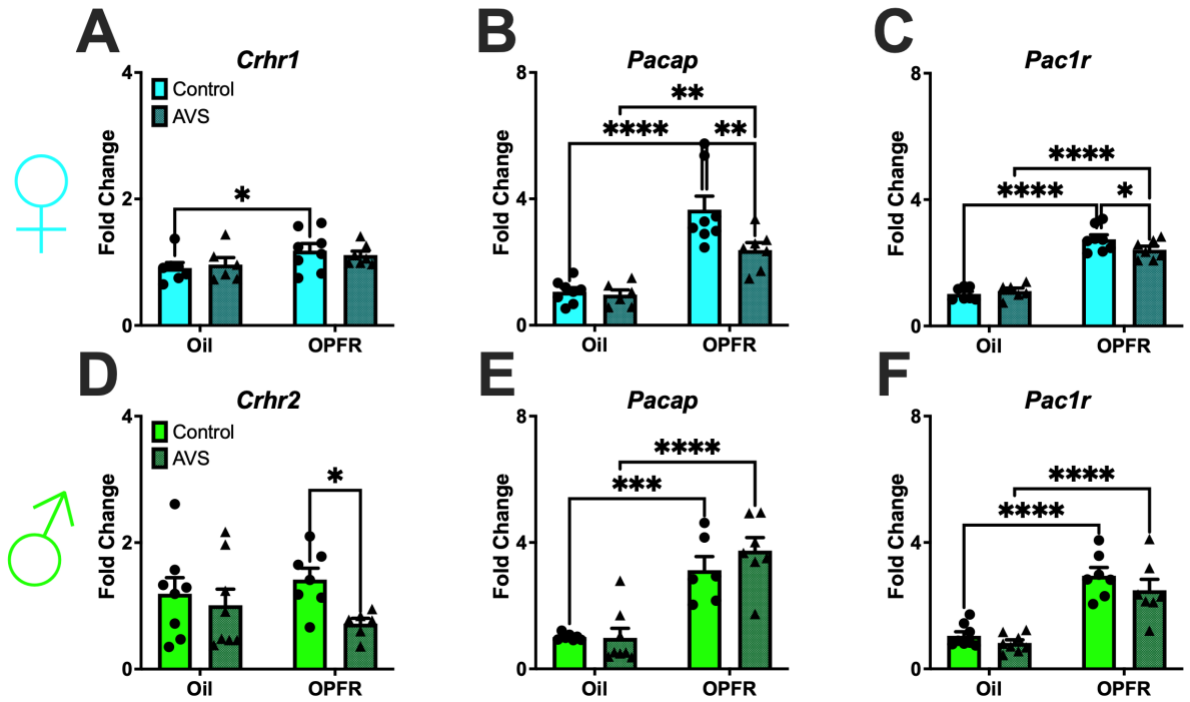

Figure 7. Bed nucleus stria terminalis (BNST) mRNA expression. Female adult offspring: (A) *Crhr1*; (B) *Pacap*; and (C) *Pac1r*. Male adult offspring: (A) *Crhr2*; (B) *Pacap*; and (C) *Pac1r*. Data are represented as mean ± SEM and dots represent the sample size (number of litters) per treatment and exposure. (*= P<0.05, **= P<0.01, ***= P<0.001, ****= P<0.0001).

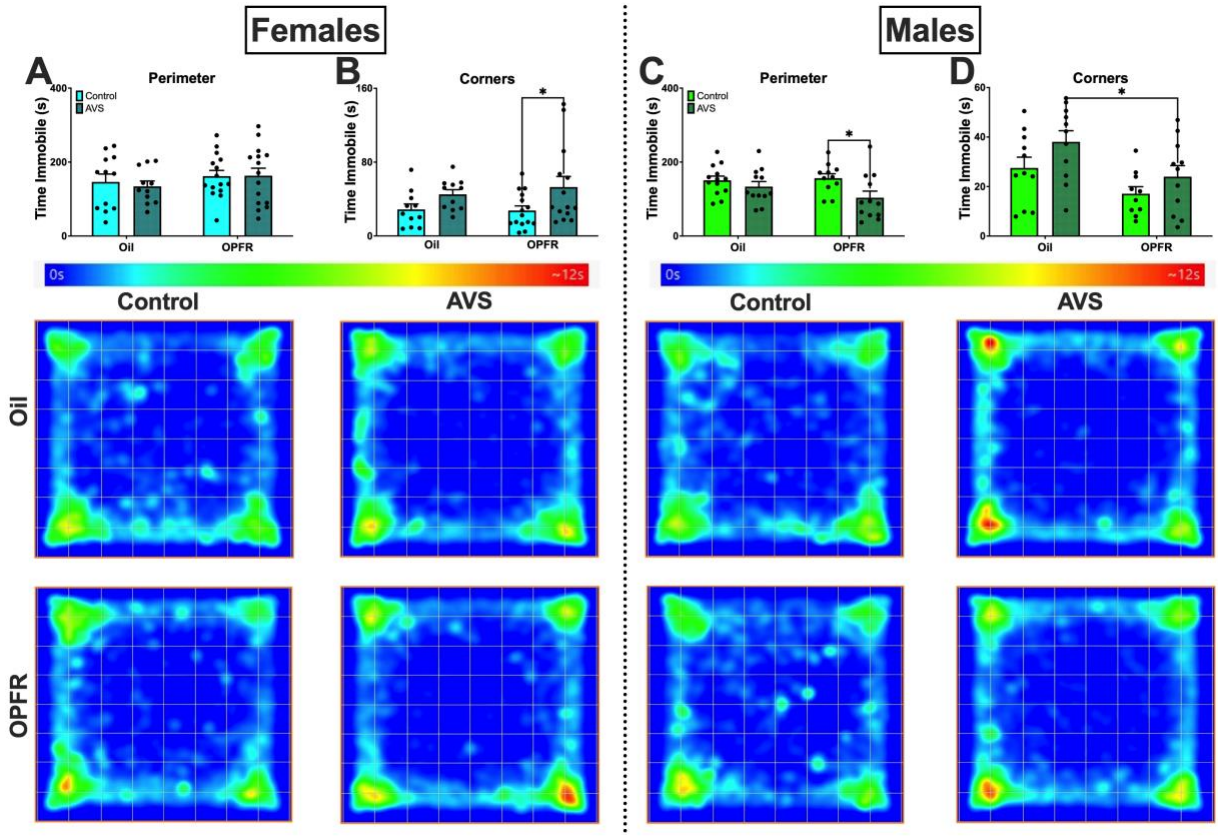

Figure 8. Open Field Test (OFT)- time immobile in the perimeter and corners for female (A and B) and male (C and D) adult offspring. Data are represented as mean ± SEM and dots represent the sample size (number of litters) per treatment and exposure. (*= P<0.05). Heat maps for each treatment and exposure group were generated by ANY-maze based on the animal's center point for the entire duration of the test, with the hottest point (in red) indicating maximum amount of time spent in an area.

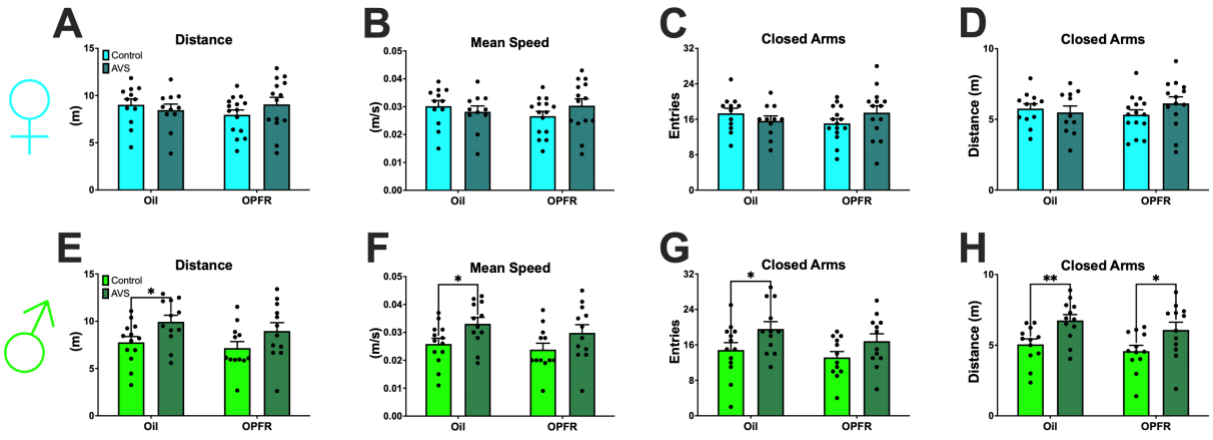

Figure 9. Elevated Plus Maze (EPM) results for female/male adult offspring: (A/E) Distance; (B/F) Mean speed; (C/G) Entries into closed arms; and (D/H) distance traveled in closed arms. Data are represented as mean ± SEM and dots represent the sample size (number of litters) per treatment and exposure. (*= P<0.05, **= P<0.01).

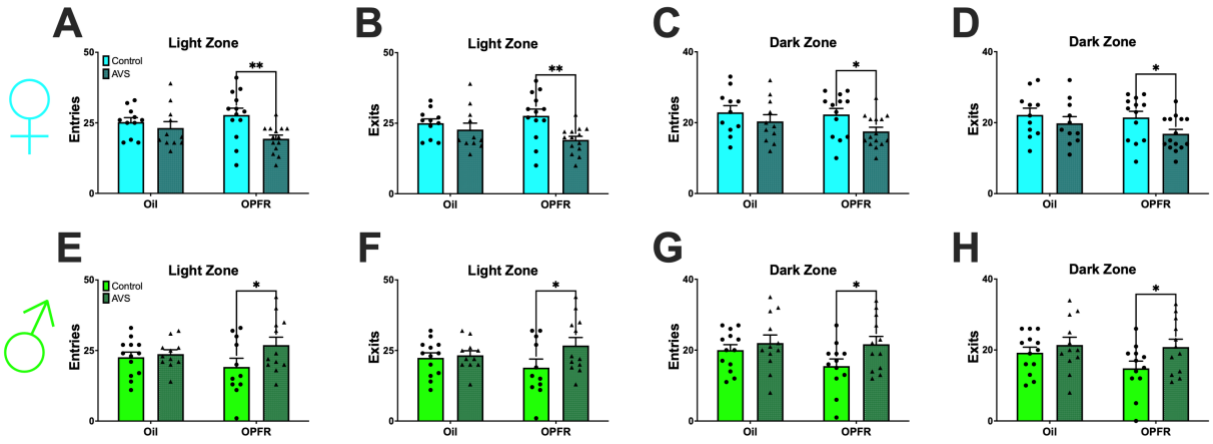

Figure 10. Light/dark box (LDB) emergence test- light and dark zone activity. Female/male adult offspring: (A/E) Entries into light zone; (B/F) Exits from light zone; (C/G) Entries into dark zone; (D/H) Exits from dark zone. Data are represented as mean ± SEM and dots represent the sample size (number of litters) per treatment and exposure. (*= P<0.05, **= P<0.01).

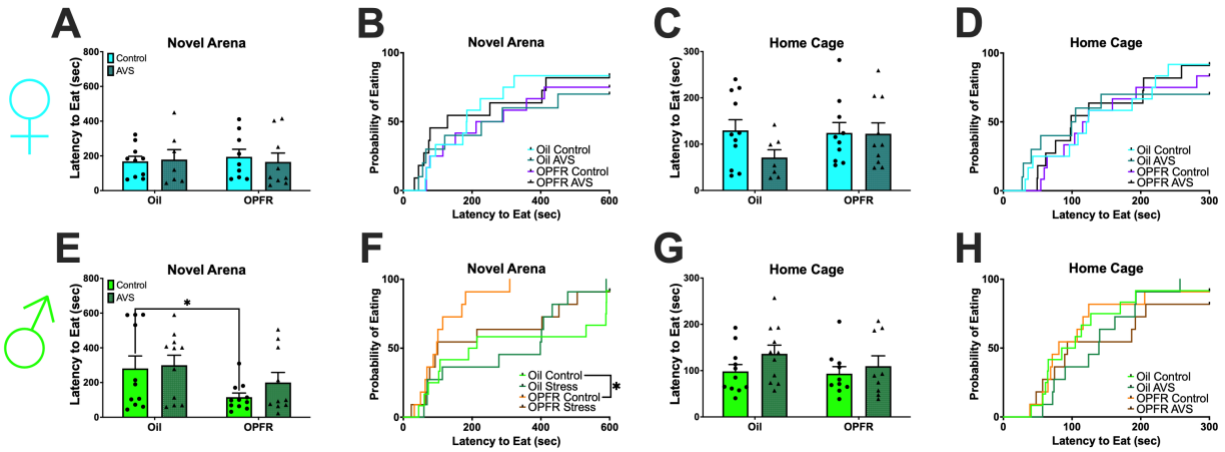

Figure 11. Novelty-suppressed feeding (NSF) for female/male adult offspring: (A/E) Latency to eat in the novel arena; (B/F) Kaplan-Meier survival curve for the probability to eat in the novel arena; (C/G) Latency to eat in the home cage; (D/H) Kaplan-Meier survival curve for the probability to eat in the home cage. Data are represented as mean ± SEM and dots represent the sample size (number of litters) per treatment and exposure.

1060

1061

1062 **Supplemental Tables/Figures**

1063

1064 **Table S1.** List of primers for qPCR.

Gene	Accession #	Forward Primer	Reverse Primer
Actb	NM_007393.3	GCCCTGAGGCTCTTTTCCA	TAGTTTCATGGATGCCACAGGA
Crh	NM_205769.2	AGGAGGCATCCTGAGAGAAGT	CATGTTAGGGGCGCTCTC
Crhr1	NM_001430903.1	CGCAAGTGGATGTTCGTCT	GGGGCCCTGGTAGATGTAGT
Crhr2	NM_001288620.1	AAGCTGGTGATTTGGTGGAC	GGTGGATGCTCGTAACTTCG
Gapdh	NM_008084.2	TGACGTGCCGCCTGGAGAAA	AGTGTAGCCCAAGATGCCCTTCAG
Hprt	NM_013556	GCTTGCTGGTGAAAAGGACCTCTCGAAG	CCCTGAAGTACTCATTATAGTCAAGGGCAT
Ikk	NM_001159774.1	CCATATCCTGGCTGTCACCT	GGCACCTTGGATGACCTAGA
Pacap	NM_001409528.1	CAGAAGGCCAGTCACCTCTGTC	GAGAGTAGGCGAGCAGCCAAAG
Pac1r	NM_133511	AACGACCTGATGGGACTAAAC	CGGAAGCGGCACAAGATGACC
Pomc	NM_008895	GGAAGATGCCGAGATTCTGC	TCCGTTGCCAGGAAACAC
Ptpn5	NM_013643.2	GCACTGTGGCCGACTTTTG	CTGCACGGTGATCTCCACG

1065

1066

1067

1068

1069

1070

1071

1072

1073

1074

1075 **Table S2.** List of primers for qPCR ordered from Bio-Rad.

Gene	Assay ID
Cyp11a1	qMmuCID0005308
Cyp11b1	qMmuCID0019988
Cyp11b2	qMmuCED0045612
Cyp21a1	qMmuCED0001670
Dbh	qMmuCID0018644
Mc2r	qMmuCID0007182
Nr3c1	qMmuCID0016200
Pnmt	qMmuCED0048695

1076

1077

1078

1079

1080

1081

1082

1083

1084

1085

1086

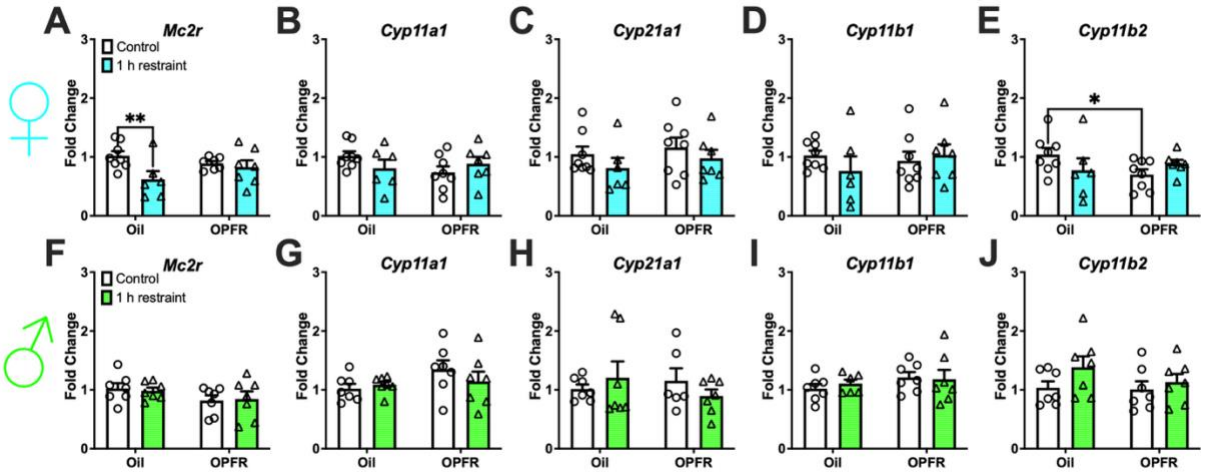

Figure S1. Adrenal mRNA expression- steroidogenic pathway. Female/male adult offspring: (A/F) *Mc2r*; (B/G) *Cyp11a1*; (C/H) *Cyp21a1;* (D/I) *Cyp11b1*; and (E/J) *Cyp11b2.* Data are represented as mean ± SEM and dots represent the sample size (number of litters) per treatment and exposure. (*= P<0.05, **= P<0.01).

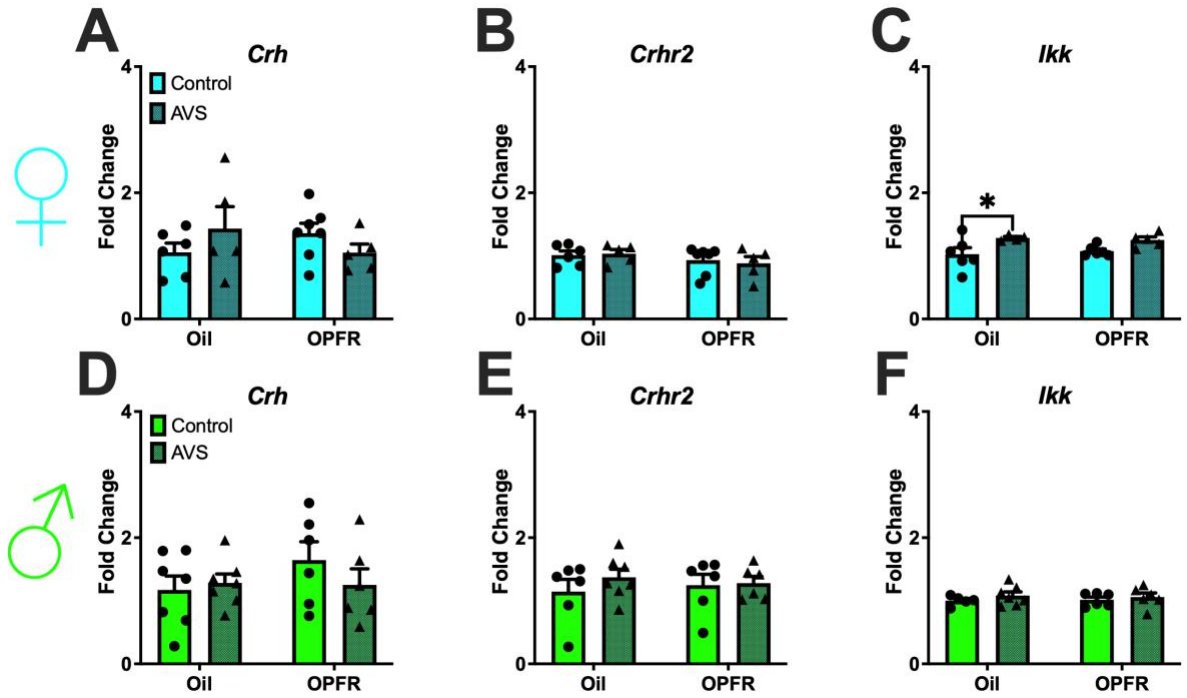

Figure S2. PVN mRNA expression. Female/male adult offspring: (A/D) *Crh*; (B/E) *Crhr2*; and (C/F) *Ikk.* Data are represented as mean ± SEM and dots represent the sample size (number of litters) per treatment and exposure. (*= P<0.05).

1118

1119

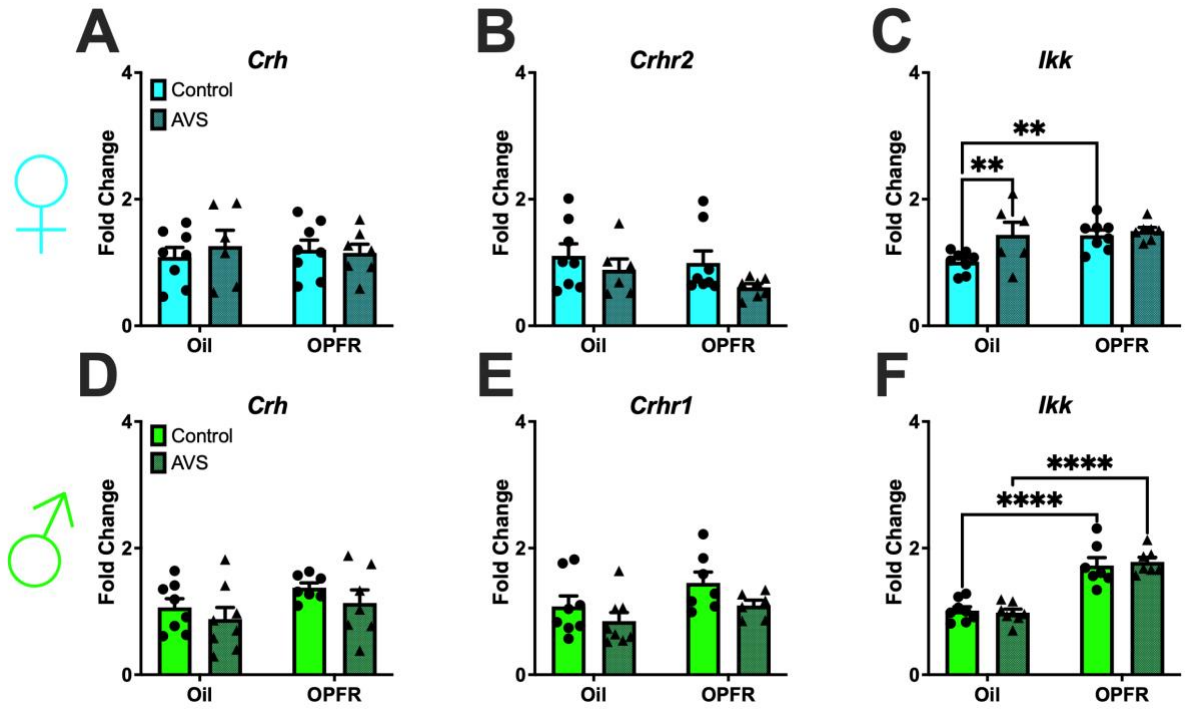

1120

1121 **Figure S3.** BNST mRNA expression. Female adult offspring: (A) *Crh*; (B) *Crhr2*; and (C) *Ikk.*

1122 Male adult offspring: (D) *Crh*; (E) *Crhr1*; and (F) *Ikk* Data are represented as mean ± SEM and

1123 dots represent the sample size (number of litters) per treatment and exposure. (**= P<0.01,

1124 ****= P<0.0001).

1125

1126

1127

1128

1129

1130

1131

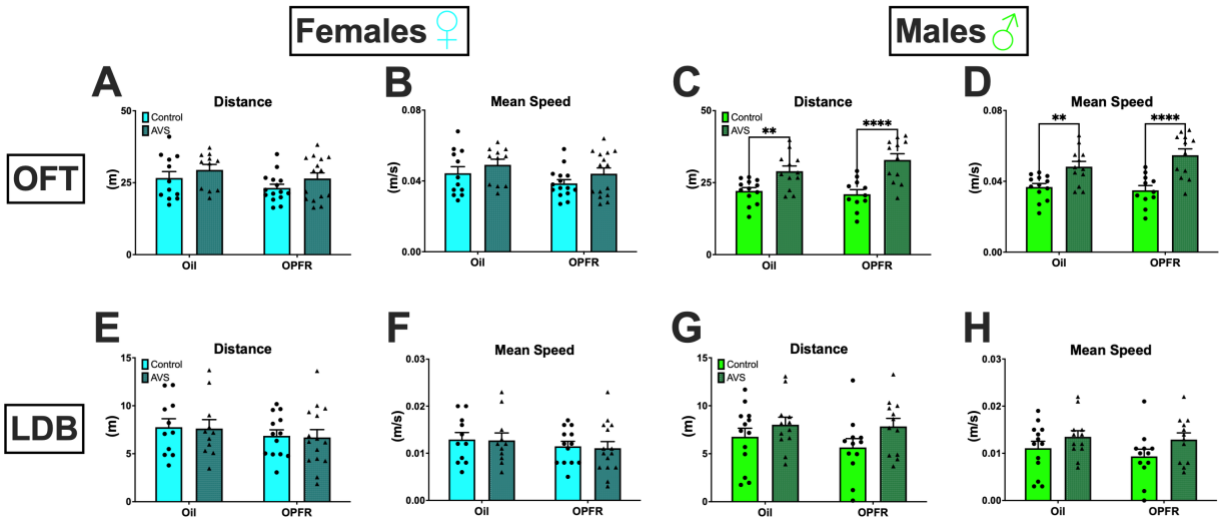

Figure S4. Behavior tests- locomotion. OFT- female/male adult offspring: (A/C) distance and (B/D) mean speed. LDB- female/male adult offspring: (E/G) distance and (F/H) mean speed. Data are represented as mean ± SEM and dots represent the sample size (number of litters) per treatment and exposure. (**= P<0.01, ****= P<0.0001).

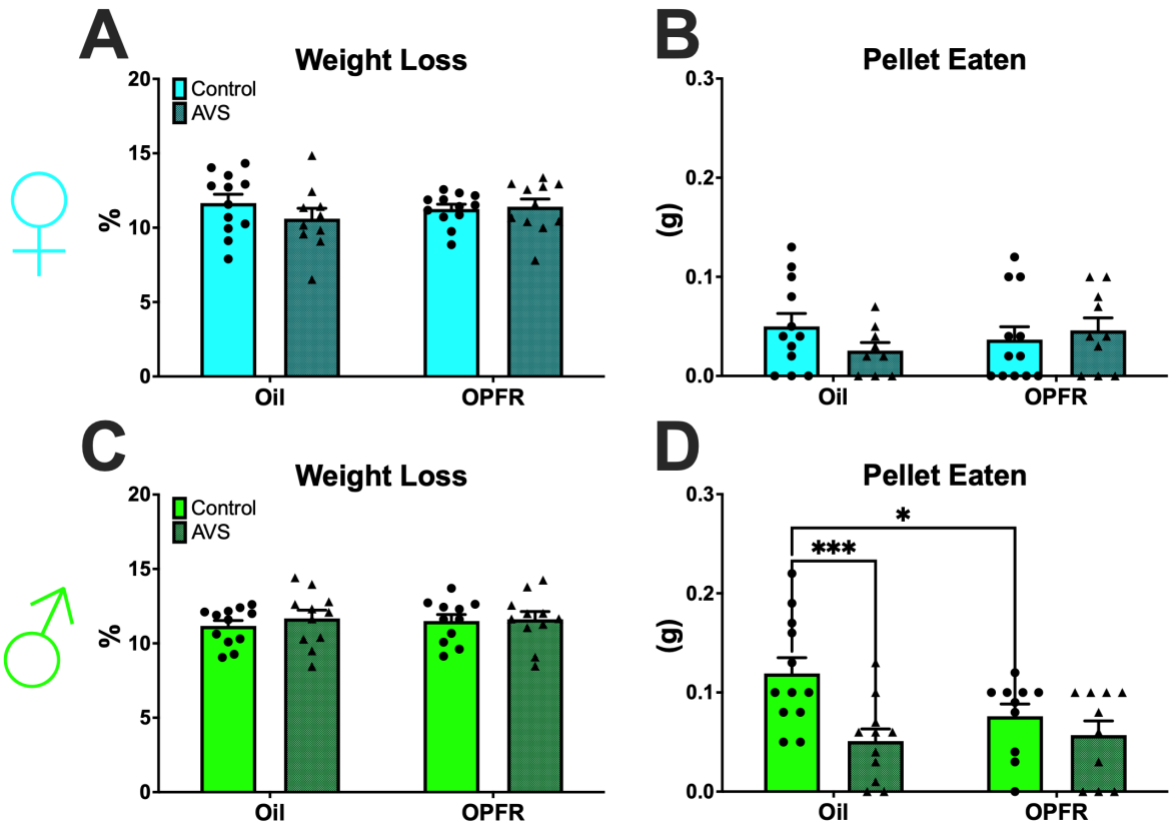

Figure S5. NSF- female/male adult offspring: (A/C) weight loss percentage and (B/D) amount of pellet eaten. Data are represented as mean ± SEM and dots represent the sample size (number of litters) per treatment and exposure. (*= P<0.05, ***= P<0.001).

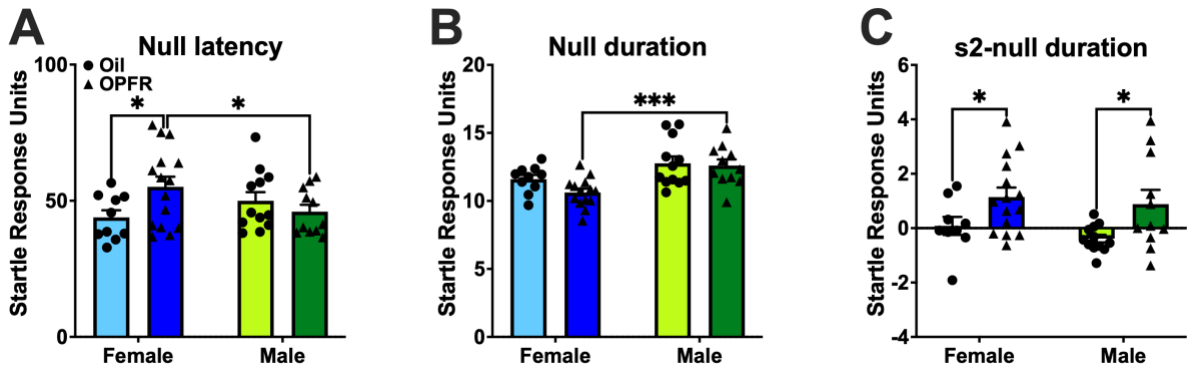

Figure S6. Startle box activity in null and S2 phase. (A) Null latency; (B) Null duration; (C) S2-null duration. Data are represented as mean ± SEM and dots represent the sample size (number of litters) per treatment and exposure. (*= P<0.05, ***= P<0.001).

1180

1181